The type IX secretion system is required for virulence of the fish pathogen Flavobacterium psychrophilum

Paul Barbier, Tatiana Rochat, Haitham H Mohammed, Gregory D Wiens, Jean-François Bernardet, David Halpern, Éric Duchaud, Mark J Mcbride

May 26, 2020

Title: The type IX secretion system is required for virulence of the fish pathogen *Flavobacterium psychrophilum*.

Authors: Paul Barbier[1], Tatiana Rochat[2], Haitham H. Mohammed[1, 3], Gregory D. Wiens[4], Jean-François Bernardet[2], David Halpern[5], Eric Duchaud[2], and Mark J. McBride[1]*

Author affiliations:

[1]Department of Biological Sciences, University of Wisconsin-Milwaukee, P. O. Box 413, Milwaukee, WI 53201

[2]Université Paris-Saclay, INRAE, UVSQ, VIM, 78350, Jouy-en-Josas, France.

[3]Department of Aquatic Animal Medicine and Management, Faculty of Veterinary Medicine, Assiut University, Assiut 71526, Egypt

[4]National Center for Cool and Cold Water Aquaculture, Agricultural Research Service, USDA, Kearneysville, WV 25430

[5]Université Paris-Saclay, INRAE, AgroParisTech, Micalis Institute, 78350, Jouy-en-Josas, France.

Paul Barbier and Tatiana Rochat contributed equally to this work. Order of these authors was determined alphabetically.

* Corresponding author: Mark J. McBride

Telephone: (414) 229-5844

Fax: (414) 229-3926

mcbride@uwm.edu

Running Title: Type IX secretion and *F. psychrophilum* virulence

ABSTRACT: *Flavobacterium psychrophilum* causes bacterial cold-water disease in wild and aquaculture-reared fish, and is a major problem for salmonid aquaculture. The mechanisms responsible for cold-water disease are not known. It was recently demonstrated that the related fish pathogen, *Flavobacterium columnare*, requires a functional type IX protein secretion system (T9SS) to cause disease. T9SSs secrete cell-surface adhesins, gliding motility proteins, peptidases, and other enzymes, any of which may be virulence factors. The *F. psychrophilum* genome has genes predicted to encode components of a T9SS. Here, we used a SacB-mediated gene deletion technique recently adapted for use in the *Bacteroidetes* to delete a core *F. psychrophilum* T9SS gene, *gldN*. The Δ*gldN* mutant cells were deficient for secretion of many proteins in comparison to wild-type cells. Complementation of the mutant with wild-type *gldN* on a plasmid restored secretion. Compared to wild-type and complemented strains, the Δ*gldN* mutant was deficient in adhesion, gliding motility, and in extracellular proteolytic and hemolytic activities. The Δ*gldN* mutant exhibited reduced virulence in rainbow trout and complementation restored virulence, suggesting that the T9SS plays an important role in the disease.

IMPORTANCE: Bacterial cold-water disease, caused by *F. psychrophilum*, is a major problem for salmonid aquaculture. Little is known regarding the virulence factors involved in this disease, and control measures are inadequate. A targeted gene deletion method was adapted to *F. psychrophilum* and used to demonstrate the importance of the T9SS in virulence. Proteins secreted by this system are likely virulence factors, and targets for the development of control measures.

54 The fish pathogen *Flavobacterium psychrophilum* is a major cause of disease and
55 mortality for aquaculture-reared salmonids, such as rainbow trout (*Oncorhynchus mykiss*) (1-3).
56 Ayu (*Plecoglossus altivelis*), European eel (*Anguilla anguilla*), and other fish are also impacted
57 by this pathogen (2-5). *F. psychrophilum* infections cause bacterial cold-water disease (BCWD),
58 which often results in erosion of the tail, destruction of tissues near the dorsal fin (saddleback
59 lesion), and systemic spread to internal organs such as the spleen and kidney. In young fish
60 mortality may occur rapidly and without obvious surface lesions, a condition sometimes referred
61 to as rainbow trout fry syndrome. *F. psychrophilum* infections are a challenge to sustainable
62 aquaculture of salmonids, and result in large economic losses (6). The mechanisms used by *F.*
63 *psychrophilum* to cause disease are poorly understood and methods to prevent or control
64 outbreaks are inadequate.

65 Antibiotic treatments have been the primary method to control outbreaks of BCWD (2,
66 7). The expense of such treatments, the danger of development of resistant strains, and the
67 potential spread of antibiotic resistance genes to other bacteria make this a poor solution.
68 Vaccine development has been complicated by the need to protect young fry that may not have
69 fully developed immune systems, uncertainties regarding the most protective antigens, and the
70 need to efficiently administer the vaccine to large numbers of fish (6). Bacteriophages are
71 promising tools to control outbreaks, but additional studies are needed to determine if this
72 approach will be broadly successful (8). Rainbow trout lines resistant to *F. psychrophilum* have
73 also been developed and used to control the disease (9-11). Improved understanding of the
74 mechanisms used by *F. psychrophilum* to cause disease could aid the continued development of
75 these and other measures to prevent or control BCWD outbreaks.

Previous studies identified *F. psychrophilum* genes and proteins that may be involved in disease. Peptidases, and other secreted enzymes, and cell-surface adhesins are suspected to be involved (1, 2, 12, 13). *F. psychrophilum* gliding motility, which allows cells to crawl over surfaces, has also been suggested as a potential virulence factor (7, 14). Genome analyses suggest that *F. psychrophilum* uses the type IX secretion system (T9SS) to secrete many proteins to the cell surface and beyond (15, 16). T9SSs are common in, but apparently confined to, members of the phylum *Bacteroidetes* (16-20). T9SSs secrete cell-surface adhesins, and soluble or cell-associated peptidases, nucleases, and other hydrolytic enzymes. T9SSs also secrete motility adhesins to the cell surface and are thus required for gliding motility (21-23). These adhesins are propelled along the cell surface by the rest of the gliding motility machinery, resulting in cell movement (24). Core components of the T9SS include the cytoplasmic membrane proteins GldL and GldM, the periplasmic protein GldN, the lipoprotein GldK, and the outer membrane protein SprA (25-29). These proteins are thought to form an envelope spanning complex that secretes proteins through the outer membrane SprA channel (22, 25, 27). GldL and GldM have been proposed to harvest the proton gradient across the cytoplasmic membrane to power both secretion and gliding (22, 27). Additional proteins involved in secretion are associated with these core components (18-20).

Proteins secreted by the T9SS have N-terminal signal peptides that facilitate their export across the cytoplasmic membrane by the Sec system, and C-terminal domains (CTDs) that target them to the T9SS for secretion across the outer membrane (18-20). Most characterized T9SS CTDs belong to either the TIGRFAM protein domain family TIGR04183 (type A CTDs) or to TIGR04131/pfam13585 (type B CTDs) (30, 31). Type A CTDs are typically removed during or after secretion (32), but removal of type B CTDs has not been carefully examined. Some proteins

secreted by T9SS are secreted in soluble form, whereas others become covalently attached to the cell surface (17, 33-35). Genome analyses can be used to identify genes predicted to encode proteins with type A CTDs or type B CTDs, thus facilitating discovery of proteins secreted by T9SSs (30, 34). Many *Bacteroidetes* are predicted to secrete dozens to hundreds of proteins using this system, and T9SS-mediated secretion of many of these proteins has been biochemically verified (34, 36, 37).

Recent experiments demonstrate that T9SSs are required for virulence of the human pathogens *Porphyromonas gingivalis* and *Prevotella melanogenica*, the fish pathogen *Flavobacterium columnare*, and the bird pathogen *Riemerella anatipestifer* (17, 21, 38-41). In each case, disruption of a gene encoding a core component of the T9SS resulted in secretion defects and loss of virulence. Proteins secreted by the T9SSs of each of these organisms are thus potential virulence factors. The role of core components of the *F. psychrophilum* T9SS in virulence has not been directly explored, but mutations in *gldD* and *gldG* that disrupted gliding motility and virulence also impacted the T9SS (14).

Methods to genetically manipulate *F. psychrophilum* have been developed (42, 43). These include replicative plasmids, transposons, and methods to make site directed insertions or deletions by homologous recombination. Genetic manipulations remain challenging however, at least in part because of the low frequencies of gene transfer into *F. psychrophilum* (42). This is especially challenging for the gene deletion approach described above, which requires multiple rounds of gene transfer (43). Another method to construct gene deletions was recently developed for *F. columnare* (44), and modified for use in many other *Bacteroidetes* (45). This method involves cloning regions upstream and downstream of the target gene into a plasmid that cannot replicate in members of the *Bacteroidetes*. The plasmid is introduced into the bacterium and gene

122 deletion occurs as a result of two recombination events between the regions on the plasmid and
123 the identical sequences on the chromosome. The plasmid carries an antibiotic resistance gene that
124 allows selection for the first recombination (integrating the plasmid into the chromosome) and
125 *sacB*, which confers sensitivity to sucrose, allowing selection for the second recombination (45,
126 46). Here we describe the use of this system to construct an *F. psychrophilum gldN* deletion
127 mutant, and demonstrate the importance of the T9SS for *F. psychrophilum* virulence.
128
129 **RESULTS**
130
131 **The *F. psychrophilum* T9SS and predicted T9SS-secreted proteins.** Analysis of the *F.*
132 *psychrophilum* strain OSU THCO2-90 genome (47) revealed each of the T9SS components
133 (Table S1), as previously reported for other *F. psychrophilum* strains (15-17). Most known
134 proteins that are secreted by T9SSs have CTDs that belong to either TIGRFAM protein family
135 TIGR04183 (type A CTDs) or TIGR04131/pfam13585 (type B CTDs). We examined the 2344
136 predicted *F. psychrophilum* strain OSU THCO2-90 proteins and identified 49 proteins predicted
137 to be secreted by the T9SS. Thirty-nine of these had type A CTDs (Table 1) and ten had type B
138 CTDs (Table 2). This probably underestimates the number of T9SS-secreted proteins, because
139 some proteins secreted by T9SSs have novel CTDs that are not easily assigned to either the type
140 A or type B CTD families (33). Included in the 49 predicted secreted proteins are nine predicted
141 peptidases, two predicted nucleases, one predicted lipase, one predicted glycoside hydrolase, and
142 28 potential adhesins, any of which may contribute to virulence. The 28 potential adhesins
143 include 17 that contain leucine-rich repeats (LRR) and are encoded by tandemly organized genes
144 (Table 1). These LRR proteins are similar to *Bacteroides forsythus* BspA and *Treponema*

145 *denticola* LrrA, which are proposed to be involved in attachment to host cells (48, 49). One of
146 the non-LRR adhesins, SprB, is involved in gliding motility in related bacteria (50).
147 *Flavobacterium johnsoniae* SprB is propelled along the cell surface, resulting in cell movement
148 (24, 50). SprB-mediated gliding of *F. psychrophilum* cells over and through fish mucus and
149 tissues may be important for virulence. The 49 predicted T9SS-secreted proteins are highly
150 conserved in other *F. psychrophilum* strains. Orthologs of each protein were present in the three
151 additional *F. psychrophilum* strains that we examined, JIP 02/86, CSF-259-93, and the type
152 strain ATCC 49418^T (12, 13, 51).
153 Previous studies of *F. johnsoniae* revealed general features of T9SS-secreted proteins
154 (30) that we examined here for *F. psychrophilum*. As with *F. johnsoniae*, *F. psychrophilum*
155 proteins with type B CTDs were typically much larger than those with type A CTDs (Tables 1
156 and 2). The median sizes of proteins with type A CTDs and type B CTDs were 46.0 kDa and
157 179.5 kDa respectively, and the largest proteins with type A CTDs and type B CTDs were 142.1
158 kDa and 366.8 kDa respectively. As for *F. johnsoniae*, many *F. psychrophilum* proteins with
159 type A CTDs are predicted or known to have enzymatic functions, whereas this was not the case
160 for any proteins with type B CTDs (Tables 1 and 2). Instead, many of the type B CTD proteins
161 are suspected to be cell surface adhesins, at least one of which (SprB) is likely involved in
162 gliding motility.
163 *F. johnsoniae* proteins with type B CTDs require the assistance of additional outer
164 membrane proteins that belong to the PorP/SprF protein domain family TIGR03519 for secretion
165 by the T9SS (30, 52). In many cases these PorP/SprF-like proteins are specific for individual
166 secreted proteins. *F. johnsoniae* SprB, for example, requires co-expression with SprF for its
167 secretion. PorP/SprF-like proteins are often encoded by the genes immediately downstream of

those encoding their cognate type B CTD-containing secreted proteins. *F. psychrophilum* strain OSU THCO2-90 has seven *porP*/*sprF* like genes (Tables S1 and S2), and six of these lie immediately downstream of genes encoding type B CTD proteins. This synteny suggests that, as for *F. johnsoniae*, these six *F. psychrophilum* type B CTD proteins may each require their cognate PorP/SprF-like proteins for secretion. The remaining four type B CTD proteins may use the 'orphan' PorP/SprF protein, THC0290_0614, although other possibilities exist. Three of the *F. psychrophilum porP*/*sprF* genes lie immediately upstream of, and are transcribed in the same direction as, genes encoding predicted peptidoglycan-binding proteins related to *P. gingivalis* PG1058, which is required for T9SS function (53). These proteins share similarity to the C-terminal peptidoglycan-binding domain of *Escherichia coli* OmpA (54, 55). The secreted type B CTD proteins, PorP/SprF-like proteins, and PG1058-like proteins may form cell-surface complexes, as predicted for similar *F. johnsoniae* proteins (30).

***sacB*-mediated deletion of the *F. psychrophilum* T9SS gene *gldN*.** To investigate the role of the T9SS in *F. psychrophilum* virulence, we deleted *gldN*, which is essential for T9SS function in related bacteria (17, 21, 56). Regions upstream and downstream of *gldN* of approximately three-kbp in size were amplified by PCR, inserted into the *sacB*-containing suicide vector pYT313 (45) and introduced into *F. psychrophilum* strain OSU THCO2-90 by conjugation. Selection for erythromycin resistance resulted in 123 colonies. These had the plasmid inserted in the genome by homologous recombination either upstream or downstream of *gldN*. Three colonies were streaked for isolation, and then grown in broth culture without selection to allow a second recombination event, resulting in loss of the inserted plasmid. These cultures were selected for sucrose resistance, and hundreds of colonies lacking the plasmid were obtained. Plasmid loss was expected to result in approximately equal numbers of wild-type

191 colonies and *gldN* deletion mutant colonies, depending on whether the second recombination
192 occurred on the same side of *gldN* as the first recombination or on the opposite side, respectively.
193 PCR analyses using primers flanking *gldN* were used to identify deletion mutants. Of eleven
194 independent sucrose resistant colonies examined, seven had *gldN* deleted, and the remaining four
195 had *gldN* intact and were thus wild type. One representative mutant colony (FpT13), which we
196 refer to as Δ*gldN*, was selected for further analysis.

197 **GldN is required for gliding motility and formation of spreading colonies.** GldN is
198 required for gliding motility in related bacteria (21, 56-58). Cells of wild-type *F. psychrophilum*
199 moved over agar by gliding, whereas cells of the Δ*gldN* mutant did not (Fig. 1, and Movie S1).
200 Complementation of the Δ*gldN* mutant by introduction of pBFp4, which carries *gldN*, restored
201 gliding motility. As a result of the gliding movements, cells of the wild-type and complemented
202 strains formed thin spreading colonies on 5% TYES medium (TYES diluted 20-fold) that was
203 solidified with agar (10 g/l), whereas cells of the Δ*gldN* mutant formed nonspreading colonies
204 (Fig. 2). In our experiments, the wild type formed spreading colonies on TYES agar media in
205 which all components except the agar had been diluted at least 2-fold, and all of the strains
206 formed nonspreading colonies on full-strength TYES agar (data not shown). This is consistent
207 with previous results that demonstrated that spreading *F. psychrophilum* colonies were only
208 observed on nutrient-poor media or media prepared with decreased amounts of agar (59).

209 **The *gldN* deletion mutant appears to be deficient in protein secretion.** Cell-free
210 culture fluid from wild-type, mutant and complemented strains were examined by SDS-PAGE
211 for soluble secreted proteins. The Δ*gldN* mutant cells released much less protein than did wild-
212 type or complemented cells (Fig. 3), suggesting a protein secretion defect. Samples of cell-free
213 culture fluid were examined by liquid chromatography-tandem mass spectrometry (LC-MS/MS).

214 The number of spectral counts of predicted secreted proteins detected are shown in Table 3. In
215 most cases, the Δ*gldN* mutant had far fewer spectral counts than did the wild-type or
216 complemented strains, corroborating a secretion defect in the mutant. The exceptions were
217 primarily the secreted leucine-rich repeat (LRR) proteins. All predicted LRR proteins had type A
218 T9SS CTDs, and requirement of GldN for their secretion was expected. However, LRR proteins
219 were detected in the cell-free spent culture fluid of both wild-type and mutant cells, and in some
220 cases higher amounts were detected for the culture fluid of the Δ*gldN* mutant. We do not know
221 the reason for this observation, but the Δ*gldN* mutant did not appear to have a general
222 permeability defect, as revealed by Fig. 3 and by the full LC-MS/MS data set that includes all
223 proteins detected in the cell-free spent medium (Dataset S1), which had very few spectra
224 corresponding to ribosomal proteins or other abundant cytoplasmic proteins.

225 **Deletion of *gldN* results in decreased extracellular proteolytic activity.** *F.*
226 *psychrophilum* secretes many peptidases (14). We examined wild-type, Δ*gldN* mutant, and
227 complemented strains of *F. psychrophilum* for extracellular proteolytic activity on TYESG agar
228 supplemented with casein (Fig. 4A). Wild-type and complemented strains formed clearing zones
229 around the cell growth, indicating digestion of casein, whereas the Δ*gldN* mutant did not.
230 Extracellular proteolytic activity in cell-free spent culture medium from each strain was
231 quantified using an azocasein-based assay (Fig. 4B). For wild-type and complemented strains,
232 high levels of soluble extracellular proteolytic activities that increased over time through late
233 exponential and early stationary phases of growth were detected. In contrast, extracellular
234 proteolytic activities for the Δ*gldN* mutant were low and failed to increase over time. *In vitro* cell
235 growth kinetics in TYESG broth cultures were not affected by *gldN* deletion (Fig. 4B). TYESG
236 contains tryptone (casein that has been digested by trypsin) and yeast extract, which may explain

237 the lack of requirement for high levels of secreted peptidases for growth in this medium. In
238 contrast, the lack of peptidase secretion may impair growth of Δ*gldN* mutant cells within the
239 host. Wild-type *F. psychrophilum* produces peptidases (some apparently strain dependent) that
240 digest collagen, fibrinogen, elastin and fish muscle tissue, and fish with BCWD often present
241 signs of tissue erosion (60, 61).

242 **The *gldN* deletion mutant is deficient in hemolytic activity and hemoglobin**
243 **utilization.** Hemoglobin is the most abundant reservoir of iron in vertebrates, and represents an
244 attractive nutrient source for pathogenic bacteria (62). *F. psychrophilum* infections in young
245 rainbow trout result in hemorrhagic septicemia. This bacterium lyses rainbow trout erythrocytes
246 and uses hemoglobin as an iron source for growth (63, 64). Wild-type cells grown on TYESG
247 agar supplemented with rainbow trout blood exhibited hemolytic activity whereas cells of the
248 Δ*gldN* mutant did not (Fig. 5). Hemolysis by the wild-type strain was accompanied by brown
249 coloration of the colonies, which was not observed for the Δ*gldN* mutant. The introduction of
250 *gldN* on pBFp4 into the Δ*gldN* mutant restored the phenotypic properties associated with the
251 wild-type strain, indicating that hemolysis and the brown coloration are dependent on a
252 functional T9SS. Dark colony pigmentation on blood agar occurs for other pathogenic bacteria
253 and may result from binding of hemoglobin or heme to the surface of bacterial cells. In *P.*
254 *gingivalis*, hemoglobin released following lysis of erythrocytes is digested by gingipain proteases
255 that are secreted by the T9SS. The released heme accounts for the black pigmentation of *P.*
256 *gingivalis* colonies and contributes to oxidative stress resistance (65). To evaluate the role of the
257 *F. psychrophilum* T9SS in hemoglobin utilization, wild-type and mutant strains were grown to
258 stationary phase in TYESG broth supplemented with 0.5 µM hemoglobin. Residual free heme
259 and hemoglobin were measured using a porphyrin detection method that relies on growth

stimulation of a heme-auxotrophic bacterial reporter strain (66). Stationary phase wild-type cultures resulted in minimal growth stimulation of the reporter, indicating little if any residual porphyrin in the medium (Fig. 6). In contrast, uninoculated medium, or stationary phase cultures of the Δ*gldN* mutant, stimulated growth of the reporter, indicating that little if any heme porphyrin was used by the Δ*gldN* mutant cells. Hemoglobin consumption was restored to the Δ*gldN* mutant by introduction of *gldN* on pBFp4. The results indicate that a functional T9SS is required for efficient hemoglobin utilization by *F. psychrophilum*. This may in part involve secretion of peptidases that cleave hemoglobin, releasing heme. The brown color of wild-type colonies (Fig. 5) suggests that released heme was captured by the cells. Heme was likely imported into wild-type *F. psychrophilum* cells, because it was absent in the medium after growth.

The *gldN* deletion mutant is deficient in adhesion, biofilm formation, and cell sedimentation. Wild-type *F. psychrophilum* cells adhere readily to polystyrene (67). Cells of the Δ*gldN* mutant were partially deficient in adhesion to polystyrene compared to wild-type cells or to cells of the complemented mutant (Fig. 7A). Adhesion of cells to a surface is the first step in biofilm formation, and *F. psychrophilum* is known to form biofilms on polystyrene (68, 69). The Δ*gldN* mutant was deficient in biofilm formation compared to the wild-type and complemented strains (Fig. 7B). *F. psychrophilum* cells also interact with each other, causing them to sediment from suspension (14). Wild-type and complemented Δ*gldN* mutant cells readily sedimented from suspension, whereas the Δ*gldN* mutant cells did not (Fig. 7C). The results indicate that the T9SS is involved in efficient adhesion, biofilm formation, and sedimentation, as was also suggested by analysis of *F. psychrophilum gldD* and *gldG* mutants (14). The many predicted adhesins

demonstrated to be secreted by the T9SS (Tables 1-3) may explain some of the defects in these processes, which each require adhesion, in the Δ*gldN* mutant cells.

GldN is required for virulence in rainbow trout. Wild-type, Δ*gldN* mutant, and complemented strains were examined for virulence using a rainbow trout injection challenge (70). At the dose examined (2.8×10^6 CFU/fish) intramuscular injection of the Δ*gldN* mutant caused no mortalities, whereas exposure to similar doses of the wild-type and complemented strains resulted in greater than 60% mortalities within 10 d of challenge (Fig. 8). The complemented strain was less virulent than the wild type. *F. psychrophilum* was isolated from all mortalities examined: wild-type (n=13/13 fish), and Δ*gldN* complemented with pBFp4 (n=11/11 fish).

The effect of *gldN* deletion on the virulence of *F. psychrophilum* was also investigated using an immersion model that more closely mimics the natural route of infection. Fish were bathed for 24 h in water containing wild-type, Δ*gldN* mutant or complemented strains at final concentrations of ~2×10^7 CFU/ml (Fig. 9A). Virulence was compared between the three strains by recording the mortality rates and by determining the *F. psychrophilum* bacterial loads in external (gills) and internal (spleen) organs. Five days after the immersion challenge, 93% of fish infected with the wild-type strain had died (Fig. 9B). In contrast, the cumulative mortality of fish exposed to the Δ*gldN* mutant was less than 2%, and was similar to that of the non-infected control group. Complementation with pBFp4 restored virulence to the Δ*gldN* mutant, resulting in cumulative mortality similar to that caused by the wild type. The increased time-to-death observed for fish exposed to the complemented strain compared to the wild-type strain may be a result of the increased copy number of *gldN* or of an effect of the *gldN* deletion on expression of nearby genes. Six of each group of 42 fish were arbitrarily sampled for the presence of *F.*

psychrophilum 6 h and 30 h after the end of the immersion challenge. At 30 h, *F. psychrophilum* was detected at high levels in the gills (average, 6×10^3 CFU per gill arch) and spleen (4×10^4 CFU per spleen) of all fish exposed to the wild-type strain (Fig. 9C). Strikingly, the bacterium was detected in the organs of only five out of 24 fish exposed to the Δ*gldN* mutant, and bacterial loads were significantly lower compared to fish exposed to the wild type. Bacterial loads in the spleen and gills of fish exposed to the complemented mutant were similar to those of fish exposed to the wild type. Together, the results indicate that a functional T9SS is required for full virulence of *F. psychrophilum* in rainbow trout.

DISCUSSION

F. psychrophilum is an important pathogen of aquaculture-reared salmonids and ayu and results in large economic losses for the aquaculture industry worldwide. Genetic manipulation to identify *F. psychrophilum* virulence factors has been hampered by the lack of efficient genetic tools. Here we demonstrate the usefulness of a *sacB*-mediated gene deletion system to construct mutations in *F. psychrophilum*, and we use this approach to demonstrate that the T9SS is required for virulence.

A gene deletion procedure was previously developed for *F. psychrophilum* strain OSU THCO2-90 (43). This double recombination procedure was similar to the one described here, but relied on an introduced restriction enzyme site for counter-selection against strains carrying the integrated plasmid. While the procedure allowed mutant construction, it was inefficient, presumably because of the multiple rounds of gene transfer required to introduce the integrative plasmid and later introduce the restriction enzyme-encoding plasmid. Here we used a procedure that was demonstrated to allow efficient targeted mutagenesis of other members of the genus *Flavobacterium* and phylum *Bacteroidetes* (44, 45). This procedure, adapted to *F.*

328 *psychrophilum*, required a single gene transfer event, relied on *sacB*-mediated sucrose sensitivity
329 for counterselection, and resulted in many *F. psychrophilum* gene deletion colonies. This
330 approach allows efficient targeted mutagenesis of *F. psychrophilum* strain OSU THCO2-90.
331 However, many other *F. psychrophilum* strains have resisted gene transfer (42), and additional
332 research is needed before similar studies will be possible for a diverse collection of *F.*
333 *psychrophilum* strains.

334 Genome analysis revealed *F. psychrophilum* OSU THCO2-90 genes encoding T9SS
335 components. Forty-nine proteins predicted to be secreted by this system were also identified,
336 including predicted peptidases, nucleases, adhesins, and motility proteins, any of which could
337 contribute to virulence. Each of the predicted secreted proteins were conserved across the
338 genomes of the four *F. psychrophilum* strains analyzed (OSU THCO2-90, ATCC 49418^T, JIP
339 02/86, and CSF-259-93), and many of them were identified as secreted proteins by proteomic
340 analyses (Table 3). Many of the proteins secreted by the *F. psychrophilum* T9SS were previously
341 identified as predicted virulence factors in the initial genome analysis of strain JIP 02/86 (12). Of
342 the 13 peptidases identified as potential virulence factors in that study, seven have type A CTDs
343 (FP0082, FP0086, FP0231, FP0232, FP0280, FP0281, and FP1763). Two additional peptidase-
344 encoding genes appear disrupted in strain JIP 02/86 (FP1776/FP1777 and FP1024/FP1023),
345 whereas strain OSU THCO2-90 has full length orthologous genes (THC0290_0931 and
346 THC0290_1343, respectively) encoding predicted peptidases with type A CTDs (Tables 1 and
347 3). Duchaud et al (12) also identified genes encoding 27 predicted adhesins, including 15
348 tandemly arrayed genes that encode proteins with LRRs that were similar to *B. forsythus* BspA
349 and *T. denticola* LrrA (48, 49). *F. psychrophilum* OSU THCO2-90 has 17 tandemly arrayed
350 genes encoding LRR proteins that are similar to those of strain JIP 02/86 (Table 1). Each of these

have type A CTDs (as do the strain JIP 02/86 LRR proteins), and are thus predicted to be secreted by the T9SS. Other previously predicted T9SS-secreted adhesins of strain JIP 02/86 (12), with strain OSU THCO2-90 orthologs indicated in parentheses, include the type A CTD protein FP1830 (THC0290_0878), and the type B CTD proteins FP2413 (THC0290_2338), FP0016 (THC0290_0025; SprB), and FP0595 (THC0290_1616).

GldN was originally identified as an *F. johnsoniae* gliding motility protein (57), and was later shown to be a core component of the *F. johnsoniae* and *P. gingivalis* T9SSs (17, 56). *gldN* is required for T9SS-mediated secretion in *F. johnsoniae*, *F. columnare*, and *P. gingivalis* (17, 21, 56). Similarly, as shown here, *F. psychrophilum gldN* was required for both gliding motility and T9SS function. The *gldN* mutant was nonmotile, and appeared to be deficient in secretion of many proteins, including predicted peptidases, hemolysins, and adhesins. Deletion of *gldN* greatly reduced the extracellular proteolytic and hemolytic activities of cells, and also reduced their adhesiveness and ability to form biofilms. Motility, adhesion, proteolysis, hemolysis, and ability to form biofilms have all been suggested to play roles in BCWD (1, 2, 7, 12, 13, 71). The only correlation observed between virulence (estimated by LD_{50} using intramuscular injection challenge) and these phenotypic traits in a recent study of 26 *F. psychrophilum* isolates was that the avirulent strain studied was deficient in colony spreading and exoproteolytic activity (7), suggesting a probable T9SS deficiency. Adhesins may allow initial attachment, and motility could facilitate penetration of tissues and spread of the infection. Secreted peptidases and hemolysins may digest host tissues and proteins, providing nutrients to the bacterium and/or destroying host defenses. The Δ*gldN* mutant was completely deficient in virulence in rainbow trout infected by injection or immersion. An *in vivo* adhesion defect of the Δ*gldN* mutant is suggested by the reduced recovery of *F. psychrophilum* cells from gill tissue 6 h after exposure

by immersion (Fig. 9C). Loss of secretion of enzymes, adhesins, and motility proteins, may together result in the avirulent phenotype of the mutant. The T9SS was also recently demonstrated to be critical for *F. columnare* to cause columnaris disease (21), suggesting similarities between at least some aspects of the virulence strategies employed by these related fish pathogens.

The results reported here are consistent with those obtained by Pérez-Pascual et al. (14) who examined transposon-induced motility mutants of *F. psychrophilum* for virulence. In that study, mutations in the motility genes *gldD* and *gldG* were linked to T9SS defects, resulting in reduction in extracellular proteolytic activity, adhesiveness, and virulence (14). GldD and GldG are not core T9SS components, and are absent from nonmotile bacteria that have T9SSs, such as *P. gingivalis* (16). However, recent studies of *F. johnsoniae* indicate that the gliding motility and T9SS machineries are intertwined (23), and suggest an explanation for the phenotypes of the *F. psychrophilum gldD* and *gldG* mutants. In *F. johnsoniae*, absence of motility protein GldJ results in apparent instability of the T9SS protein GldK, and thus in loss of protein secretion (23). Further, mutations in some other motility genes (including *gldD* and *gldG*) result in apparent instability of GldJ protein (72), and thus in loss of GldK and of T9SS function (23). The apparent interconnections between the motility and T9SS machineries may explain how mutations in the *F. psychrophilum* motility genes *gldD* and *gldG* perturb T9SS function.

Our results may also help to explain the lack of virulence of rifampicin resistant *F. psychrophilum* mutants that have been isolated and examined as vaccine candidates (73). The most attenuated of these strains were deficient in motility (74). Given the link between gliding motility and the T9SS described above, the mutants may have also been compromised for protein secretion, which could have contributed to the attenuated phenotype.

397 The proteomic analysis of spent cell-free culture fluid confirmed our predictions
398 regarding secretion of many proteins that carried type A or type B CTDs, but also revealed some
399 unexpected results. Numerous LRR proteins, each of which had type A CTDs, were predicted to
400 be secreted by the T9SS, but surprisingly, many of these were found at similar, or for some
401 higher, levels in the cell-free culture fluid of the Δ*gldN* mutant. The LRR proteins were predicted
402 to be cell-surface proteins (12). We do not know why similar amounts of LRR proteins were
403 found in the cell-free spent culture fluids of wild-type and Δ*gldN* mutant cells. Perhaps the LRR
404 proteins were not actually secreted in soluble form, but instead were present on the surface of, or
405 inside of, extracellular outer membrane vesicles released by wild type and mutant cells
406 respectively. Our proteomic results for secretion of LRR proteins by wild type and Δ*gldN* mutant
407 cells differ from those obtained in a similar study of wild type, *gldD*, and *gldG* mutant cells (14).
408 The *gldD* and *gldG* mutants secreted much smaller amounts of LRR proteins than did wild type
409 cells. We do not know the reasons for this difference. As discussed above, GldD and GldG, are
410 not thought to be components of the T9SS, but they impact its function. Mutations in *gldD* and
411 *gldG* may thus affect the functioning of the T9SS differently than mutations in *gldN*, which
412 encodes a core component of the system.
413 The 49 proteins with type A and type B CTDs that are predicted to be secreted by the *F.*
414 *psychrophilum* T9SS probably underestimate the actual number of proteins secreted by this
415 system, since some T9SS-secreted proteins from related bacteria have novel CTDs (33).
416 Supporting this, deletion of *gldN* appeared to disrupt secretion of many proteins that lacked
417 obvious T9SS CTDs (Dataset S1). Included among these proteins are 14 predicted peptidases
418 that may contribute to virulence. Analysis of the C-terminal regions of seven proteins that lacked
419 obvious type A or type B CTDs but that appeared to be secreted by the T9SS as indicated by

Dataset S1, and by the results of a previous study (14) revealed two putative adhesins (THC0290_0754 and THC0290_2201) and one probable peptidase (THC0290_0500) that exhibit some similarity to T9SS CTDs (Fig. S1). These may represent a novel T9SS CTD type, or may indicate that the sequence constraints delineating CTD domains may need to be relaxed to avoid false negatives. Identification of additional proteins secreted by the T9SS will not be surprising given our current limited understanding of the functioning of this system. An alternative potential explanation for the apparent T9SS-mediated secretion of some non-CTD proteins is that deletion of *gldN*, which is expected to result in the failure of numerous cell-surface proteins to reach their destination, could have pleotropic effects on the cell surface that perturb other protein secretion systems. *F. psychrophilum* has multiple predicted type I secretion systems (12) that could have been affected in this way.

Our analyses of *F. psychrophilum* motility proteins SprC and SprD identified some unexpected features that were not immediately obvious from earlier studies. *F. johnsoniae* SprC was not previously recognized as a potential T9SS-secreted protein (30, 52). *F. psychrophilum* SprC also fell below the trusted cutoff for inclusion in type B CTD family TIGR04131, but it had a conserved region (pfam13585; Table 2) that is found in all type B CTDs. The regions recognized by TIGR04131 and pfam13585 are nearly identical (19). Further, *sprD*, which is immediately downstream of *sprC*, encodes a protein with a PorP/SprF-like region (TIGR03519; Table S2), suggesting that it may interact with SprC and facilitate its secretion by the T9SS. Similar conserved regions are found in SprC (pfam13585) and SprD (TIGR03519) proteins of *F. columnare* and other related bacteria. *sprC*, *sprD*, *sprB*, and *sprF* appear to form an operon in *F. psychrophilum* and in many other *Bacteroidetes*, and SprC and SprD support SprB-mediated gliding motility (30, 52). As mentioned above, SprB also requires its cognate PorP/SprF-like

443 protein (SprF) for its secretion (30). The results presented here enhance our understanding of the
444 possible interactions between these four common *Bacteroidetes* gliding motility proteins, and
445 their relationships to the T9SS.

446 The *F. psychrophilum* T9SS is important for virulence, but which of the many secreted
447 proteins contribute to BCWD remains unclear. The roles of the individual secreted proteins can
448 now be examined systematically using the gene deletion approach described above. Since this
449 deletion technique does not leave antibiotic resistance genes or other foreign DNA in the mutant,
450 it can be used iteratively to generate strains lacking many genes. This is important given the
451 many potential secreted virulence factors, and should allow questions of redundancy to be
452 addressed. Construction of mutants lacking one or more critical secreted virulence factors may
453 reveal the most important mechanisms employed by *F. psychrophilum* to cause disease, and
454 could suggest control measures. Such mutants may function as attenuated vaccine strains that
455 interact with fish and generate a protective immune response, but fail to cause disease. Since
456 T9SSs are involved in diseases caused by many related animal and human pathogens (17, 21, 38-
457 41), improved understanding of *F. psychrophilum* virulence may have impacts beyond fish
458 health and sustainable aquaculture.

459 **MATERIALS AND METHODS**

460 **Bacterial strains, plasmids, and growth conditions.** *F. psychrophilum* strain OSU
461 THCO2-90 (47, 75), was the wild-type strain used in this study. *F. psychrophilum* cultures were
462 grown at 18°C in tryptone yeast extract salts (TYES) medium (76, 77), which contains per l, 4 g
463 tryptone, 0.4 g yeast extract, 0.5 g $MgSO_4 \cdot 7H_2O$, and 0.5 g $CaCl_2 \cdot 2H_2O$, pH adjusted to 7.2. For
464 some experiments TYESG, which contains per l, 4 g tryptone, 0.4 g yeast extract, 0.5 g
465 $MgSO_4 \cdot 7H_2O$, 0.2 g $CaCl_2 \cdot 2H_2O$, and 0.5 g D-glucose, pH adjusted to 7.2, was used. TYESG

differs from TYES only by the addition of glucose and by the reduced amount of $CaCl_2$. For solid media, agar was used at 15 g/l unless indicated otherwise. For most experiments, *F. psychrophilum* was recovered from -80°C freezer tubes onto TYES agar and incubated 72 hours at 18°C. Strains were streaked on fresh agar, incubated 72 hours at 18°C, and then used to inoculate 20 ml TYES broth cultures, which were incubated for 24 to 48 h at 18°C with shaking at 200 rpm. Extracellular proteolytic activity on solid medium was visualized using TYESG agar supplemented with 7.5 g casein (Sigma-Aldrich Ref. C8654) per l or 10 g hemoglobin (Hb; Sigma-Aldrich Ref. 08449) per l. Hemolysis and colony pigmentation were visualized on TYESG agar supplemented with 50 ml rainbow trout blood per l. Blood was collected by caudal venipuncture of anesthetized rainbow trout and immediately mixed with heparin at a final concentration of 250 IU/ml (Heparine Choay® 25000 IU/5 ml injectable solution, Sanofi Aventis) at 4°C. Colony spreading was examined on 5% TYES (TYES with all components diluted 20-fold) solidified with 10 g agar per l.

Bacteroides thetaiotaomicron VPI-5482^T (78) was grown in Difco^{TM} M17 medium #218561 (Becton Dickinson, Sparks, MD), supplemented with (per l) 5 g glucose, 0.5 g cysteine, and 6 g agar, and is referred to here as M17-glu. *E. coli* strains were grown in lysogeny broth (LB) at 37°C (79). Strains and plasmids used in this study are listed in Table 4 and primers are listed in Table 5. Antibiotics were used at the following concentrations when needed: ampicillin, 100 µg/ml; erythromycin, 10 µg/ml.

Conjugative transfer of plasmids into *F. psychrophilum*. Plasmids were transferred from *E. coli* S17-1 λ-*pir* into *F. psychrophilum* strains by conjugation. Briefly, *E. coli* strains were incubated overnight with shaking in LB at 37°C. *F. psychrophilum* strains were incubated 30 h with shaking in TYES broth at 18°C. Cells were collected by centrifugation at 3220 × g for

25 min, washed twice with 1 ml TYES and suspended in 500 µl TYES. The suspensions of *E. coli* and *F. psychrophilum* cells were mixed, spotted on TYES agar and incubated at 18°C for 48 hours. The cells were removed from the plate with a scraper and suspended in 2 ml TYES. 100-µl aliquots were spread on TYES agar containing 10 µg erythromycin per ml and incubated at 18°C for 5 to 7 days.

Construction of the *gldN* deletion mutant. To delete *F. psychrophilum gldN* (THC0290_0743), a 2,858-bp fragment spanning the last 387 bp of *gldK* (THC0290_0740), *gldL* (THC0290_0741), *gldM* (THC0290_0742) and including the first 141 bp of *gldN* was amplified using Phusion DNA polymerase (New England Biolabs, Ipswich, MA) and primers 2060 (introducing a BamHI site) and 2061 (introducing a SalI site). The fragment was digested with BamHI and SalI and ligated into the suicide vector pYT313, which had been digested with the same enzymes, to generate pBFp0. A 3,132-bp fragment spanning the final 153 bp of *gldN*, THC0290_0744, THC0290_0745 and the first 1,220 bp of THC0290_0746 was amplified with primers 2062 (introducing a SalI site) and 2063 (introducing an SphI site). The fragment was digested with SalI and SphI and inserted into pBFp0 that had been digested with the same enzymes, to generate the deletion construct pBFp1. pBFp1 was transferred by conjugation into *F. psychrophilum* OSU THCO2-90, and colonies that had the plasmid integrated into the chromosome by recombination were obtained by selecting for erythromycin resistance. Resistant colonies were streaked for isolation on TYES agar containing erythromycin. An isolated colony was used to inoculate 10 ml TYES broth without erythromycin, which was incubated for 30 h at 18°C to allow loss of the integrated plasmid. Recombinants that had lost the plasmid were selected by plating on TYES containing 50 g/l sucrose, and incubating at 18°C. Isolated sucrose-resistant colonies were picked and streaked for isolation on TYES agar containing sucrose to

512 eliminate background cells that had not lost the plasmid. Colonies were screened by PCR using
513 primers 2076 and 2077, which flank *gldN* to identify the *gldN* deletion mutant. Streaking
514 colonies for isolation on selective media at both the plasmid integration (erythromycin selection)
515 and plasmid loss (sucrose selection) steps was critical to eliminate nonselected cells.

516 **Complementation of the *gldN* deletion mutant.** A plasmid carrying *F. psychrophilum*
517 *gldN* was constructed using shuttle vector pCP11 (80). Primers 2076 (introducing a KpnI site)
518 and 2077 (introducing an SphI site) were used to amplify a 1,161 bp product spanning *gldN*. The
519 product was digested with KpnI and SphI and ligated into pCP11, which had been digested with
520 the same enzymes, to generate pBFp4, which was transferred into *F. psychrophilum* by
521 conjugation.

522 **Analysis of colony spreading and cell motility.** *F. psychrophilum* wild-type, Δ*gldN*
523 mutant, and complemented strains were serially diluted and plated on 5% TYES (TYES diluted
524 20-fold) solidified with 10 g agar per l. The plates were incubated for 32 h at 18°C to obtain
525 isolated colonies. Colonies were examined using a Photometrics Cool-SNAP$_{cf}^2$ camera mounted
526 on an Olympus IMT-2 phase-contrast microscope. Colonies were also obtained by spotting 5 µl
527 of cells at OD_{600} of 1.5 on 5% TYES solidified with 10 g agar per l and incubating for 12 d at
528 18°C, and these were examined macroscopically using a Nikon D7200 camera. Motility of
529 individual cells on agar was examined by spotting cells on a pad of full-strength TYES solidified
530 with 10 g agar per l on a glass slide, allowing the spot to dry briefly, and covering it with an O_2-
531 permeable Teflon membrane (Yellow Springs Instrument Co., Yellow Springs, OH) that
532 prevented dehydration and served as a coverslip. Cell movements over agar were observed using
533 an Olympus BH-2 phase-contrast microscope. Images were recorded using a Photometrics Cool-
534 SNAP$_{cf}^2$ camera and analyzed using MetaMorph software (Molecular Devices, Downingtown,

535 PA). Rainbow traces of cell movements were made using ImageJ version 1.45s
536 (http://rsb.info.nih.gov/ij/) and macro Color FootPrint (24).

537 **Analysis of secreted proteins by SDS-PAGE and LC-MS/MS.** *F. psychrophilum* wild-
538 type, Δ*gldN* mutant, and complemented mutant were grown in TYES broth at 18°C for
539 approximately 48 h. Growth was monitored with a Klett-Summerson colorimeter (Klett
540 Manufacturing Co., Inc. Long Island City, New York) and cultures were harvested in early
541 stationary phase when the Klett readings reached 160. Cultures were centrifuged at 16,873 × g
542 for 10 min at 4°C. The fluid was filtered with 0.45 µm pore size HT Tuffryn filters (PALL Life
543 Sciences). Proteins were precipitated by mixing 1 volume of trichloroacetic acid (TCA) with 9
544 volumes of cell-free spent culture fluid, incubating at -20^{o}C for 1 h, and centrifuging for 45 min
545 at 12,210 × g at 4^{o}C. The pellet was washed with acetone (0^{o}C) and centrifuged for 10 min at
546 12,210 × g to collect the pellet, which was dried for 10 min at room temp. Proteins were
547 suspended in SDS-PAGE loading buffer, boiled for 10 min, and were separated by SDS-PAGE
548 (81) using a 12% polyacrylamide gel, and detected using the BioRad (Hercules, CA) silver stain
549 kit. Protein pellets (TCA-precipitated from cell-free spent culture fluid and acetone-washed as
550 above) were also analyzed directly by enzymatic digestion and nano-LC-MS/MS at the
551 University of WI-Madison Mass Spectrometry Facility as outlined on the website
552 (https://www.biotech.wisc.edu/services/massspec), and as described previously (21) except that
553 LC-MS/MS data were searched against proteins encoded by the *F. psychrophilum* strain OSU
554 THCO2-90 genome (47).

555 **Analysis of proteolytic activity.** Proteolytic activity was quantified using azocasein as a
556 substrate as previously described (82). Briefly, *F. psychrophilum* strains were grown in 25 ml
557 TYESG broth at 18°C and 200 rpm for 2 days. Two ml of cultures at OD_{600} of 0.5, 1.0 and 2.0

were centrifuged, the supernatants filtered using 0.22 µm Millipore filters and stored at 4°C for 24 h. For protease activity assay, a solution of 20 g azocasein per l (Sigma-Aldrich) was prepared in 0.1 M Tris-HCl pH 7.4. The cell-free supernatant (150 µl) was mixed with 150 µl azocasein solution and incubated for 4 h at 25°C. The reaction was stopped by adding 750 µl of TCA (50 g/l). The reaction mix was centrifuged at 20,000 × g for 30 min and 150 µl of the supernatant was mixed in a 96-well microplate well containing 150 µl of 1 M NaCl. The OD_{440nm} was measured using a Tecan Microplate Reader (Infinite 200 PRO) and the negative control OD_{440nm} value was subtracted from this. One unit of proteolytic activity was defined as an increase in absorbance of 0.001 under the conditions of the assay. All cultures were performed in triplicate and an average of the three experiments was used as the measure of proteolytic activity over the growth curve.

Hemoglobin utilization. The ability to use hemoglobin as a heme source was investigated by measuring the residual porphyrin (heme, hemoglobin or protoporphyrin IX) remaining after growth of *F. psychrophilum* to stationary phase in TYESG broth supplemented with 0.5 µM hemoglobin (Sigma-Aldrich Ref. H2500), using the heme-protoporphyrin IX-screen method (66). This method is a bacterial-growth-based assay that exploits the heme auxotrophy of *B. thetaiotaomicron*. Briefly, a vertical gel set-up with 0.8-cm spacers was filled with M17-glu medium containing 8×10^5 *B. thetaiotaomicron* CFU/ml. Stationary phase *F. psychrophilum* cultures in TYESG broth (with or without 0.5 µM hemoglobin) were heat-inactivated by incubation at 37°C for 3 h. The cultures (100 µl volumes) were loaded in wells of the *B. thetaiotaomicron*-containing gel and sterile TYESG broth containing 0.5 µM hemoglobin was used as a positive control. The gel was overlaid with a 5 ml agar plug (12 g/l). *B. thetaiotaomicron* growth stimulation was visualized as dense growth around wells after

581 overnight incubation at 37°C. The surface area of growth stimulation, which correlates with
582 heme concentration in the sample, was determined using ImageJ (V1.45 s; Wayne Rasband,
583 National Institute of Health, USA). The results corresponded to three independent *F.*
584 *psychrophilum* cultures.

585 **Adhesion, biofilm, and sedimentation assays.** Adhesion to polystyrene, biofilm
586 formation on polystyrene, and cell sedimentation were determined as previously described (14)
587 except that cells were grown in TYES instead of TYESG for the adhesion assay, and in half-
588 strength TYES instead of half-strength TYESG for the biofilm and sedimentation assays, as
589 outlined briefly below.

590 For the adhesion assay, cells were grown in TYES broth to OD_{600} = 0.7. One ml of each
591 culture was centrifuged at 11,000 × g for 5 min, the supernatant was removed, and cell pellets
592 were suspended in 1 ml sterile distilled water. One hundred microliters of each strain suspension
593 was added to a 96-well microtiter polystyrene plate with flat bottom (NunclonTM Delta surface,
594 ThermoFisher Scientific, Waltham, MA) and sterile water was used as a negative control in non-
595 inoculated wells. The plate was incubated at 18^{o}C for 3 h without shaking. Subsequently, wells
596 were washed twice with sterile distilled water and the adherent cells were stained with 100 µl of
597 crystal violet (10 g/l) for 30 min at room temperature. The wells were washed four times with
598 sterile distilled water, and 100 µl of absolute ethanol was added to each well to solubilize the
599 remaining crystal violet. Cell adhesion was determined by measuring OD_{595} using a CLARIOstar
600 Microplate Reader (BMG Labtech, Ortenberg, Germany). The level of adhesion observed for
601 each strain was compared with the adhesion of the wild-type strain, which was set as 100. All
602 assays were performed in quadruplicate and repeated at least two times. The absorbance of the
603 negative control was subtracted from the absorbance of each strain.

For biofilm formation, cells were grown in half-strength TYES broth to the mid-exponential phase. The cultures were diluted 1:100 in half-strength TYES broth and 150 µl of each diluted bacterial culture was deposited in wells of 96-well flat bottom polystyrene microtiter plates. The plates were covered with aluminum foil and incubated in a humid environment at 18°C under static conditions for 120 h. Biofilm development was evaluated in four wells per strain, and wells containing sterile non-inoculated medium were used as negative controls. The culture fluid was discarded, the wells were washed twice with 200 µl of sterile distilled water. 150 µl of crystal violet (10 g/l) was added to each well and incubated at room temperature for 30 min. Unbound stain was removed by washing the wells four times with 200 µl of sterile distilled water. Stain bound to biofilm cells was solubilized in 100 µl of ethanol and the absorbance (OD_{595} nm) was determined.

To measure bacterial cell sedimentation, cells were grown in half-strength TYES broth at 18°C, 200 rpm for 96 h. Tubes were allowed to stand static for 10 min before being photographed.

Rainbow trout challenges. Two experimental infection models differing by the infection route (injection or immersion), size of fish, and lines of fish were used. For the intramuscular injection model, fish (27.5 g average mass) of the ARS-Fp-C line were used, which are intermediate in resistance (83). Four groups of 20 fish (n=80) were anesthetized and challenged with each *F. psychrophilum* strain by intramuscular injection at a point midway between the insertion of the dorsal fin and the lateral line. Injection of 25 µl was performed using a 26 g needle attached to an Eppendorf repeating syringe. All challenge fish were maintained using flow-through spring water. Two groups of 20 fish were injected with sterile PBS, as a negative control. CFU counts (triplicate dilution series) for wild type were 2.6 (± 0.8) × 10^6, Δ*gldN*

627 mutant 2.7 (± 1.3) × 10^6 and Δ*gldN* complemented mutant 2.8 (± 1.5) × 10^6 CFU/fish. The water
628 temperature during challenge was 13.2°C. Mortalities were recorded daily and examined for
629 clinical signs of disease and for the presence of *F. psychrophilum*.
630 For the bath immersion challenge the rainbow trout (*O. mykiss*) homozygous line A36
631 was used as previously described (84, 85). The uniformity of genetic background in isogenic
632 lines and the high susceptibility of line A36 to *F. psychrophilum* infection makes this line useful
633 to examine bacterial virulence (14). Fish were reared at 10°C in dechlorinated recirculated water
634 until they reached 1.4 g, and were then transferred to continuous flow aquaria for infection
635 experiments. Bacteria used for infections were prepared as follows: wild type, Δ*gldN*, and Δ*gldN*
636 complemented with pBFp4 were grown in TYESG broth at 200 rpm and 18°C until late-
637 exponential phase (OD_{600nm} = 1.3). The bacterial cultures were directly diluted (200 fold) into 15
638 l of aquarium water. Bacteria were maintained in contact with fish (n = 42 per group) for 24 h by
639 stopping the water flow, and were subsequently removed by restoring flow. Sterile TYESG broth
640 was used for the control group. *F. psychrophilum* bacterial counts were determined at the
641 beginning and at the end of the immersion challenge by plating serial dilutions of water samples
642 on TYESG agar. Water was maintained at 10°C under continuous aeration during the
643 experiment. Virulence was evaluated according to i) fish mortality during twelve days post-
644 infection and ii) bacterial loads in organs. Six of each group of 42 fish were randomly chosen
645 and sacrificed 6 h and 30 h after the end of the immersion challenge to evaluate the *F.*
646 *psychrophilum* bacterial load in the spleen (whole organ) and gills (one gill arch). Organs were
647 mechanically disrupted in Lysing Matrix tubes containing 400 µl of peptone (10 g/l water) and 1
648 mm ceramic beads (Mineralex SAS, Lyon, France). Samples were homogenized at 6.0 m s^{-1} for
649 two cycles of 20 s on a FastPrep-24 instrument (ThermoFisher Scientific, Waltham, MA). Serial

650 dilutions of the homogenized solution were plated on TYESG agar supplemented with fetal calf
651 serum (50 ml/l) and incubated for 3 d at 18°C. Two independent experiments were performed.
652 Statistical differences of bacterial loads between groups were analyzed using the Mann-Whitney
653 test; the Kaplan-Meier method was used to draw survival curves that were compared using the
654 Gehan-Breslow-Wilcoxon test with GraphPad Prism 8.1.2 (GraphPad Software, San Diego, CA,
655 USA).

656 **Bioinformatic analyses.** Genome sequences were analyzed for T9SS genes encoding
657 proteins that belong to appropriate TIGRFAM multiple-sequence alignment families (86). This
658 was accomplished using the Integrated Microbial Genomes (IMG version 4.0.1
659 [https://img.jgi.doe.gov/]) Function Profile Tool to examine the genomes for sequences predicted
660 to encode orthologs of GldK (TIGR03525), GldL (TIGR03513), GldM (TIGR03517), GldN
661 (TIGR03523), and SprA (TIGR04189). The genomes were also examined for genes encoding
662 proteins with type A CTDs (TIGR04183), type B CTDs (TIGR04131 and pfam13585) (19), and
663 for genes encoding PorP/SprF-like proteins (TIGR03519) in the same way. In each case, the
664 trusted cutoffs assigned by The J. Craig Venter Institute (JCVI) that allow identification of the
665 vast majority of family members with vanishingly few false positives (86) were used. Other
666 potential *F. psychrophilum* T9SS proteins listed in Table S1 (PorU, PorV, SprE, SprT, Plug,
667 PorQ, PorZ, PorX, PorY, and PG1058) were identified by BLASTP analysis using the
668 appropriate *F. johnsoniae* or *P. gingivalis* protein as query.

669 **Data Availability**

670 All data associated with this work is included either in the manuscript or in the online
671 supplemental materials.

672 **Ethics statements**

673 The immersion challenges were performed in accordance with the European Directive
674 2010/2063/UE regarding animal experiments, and were approved by the institutional review
675 ethics committee, COMETHEA, of the INRAE Center in Jouy-en-Josas, France. Authorizations
676 were approved by the Direction of the Veterinary Services of Versailles (authorization number
677 15-58). Injection challenge was performed under the guidelines of NCCCWA Institutional
678 Animal Care and Use Committee Protocol #132.
679

680 **Acknowledgements:**

681 The authors are grateful to the staff of the fish facilities (INRA IERP and PEIMA,
682 France) and to Edwige Quillet and Nicolas Dechamp (INRA GABI, France) for supplying fish
683 and advice. We thank Victor Folcher for technical help. For challenge experiments conducted at
684 the NCCCWA, we thank Timothy Leeds for providing fish, and Travis Moreland and Keira
685 Osbourn for technical help. This work was financially supported by the Agence Nationale de la
686 Recherche (grant ANR-17-CE20-0020-01 FlavoPatho), by grant MCB-1516990 from the
687 National Science Foundation to MJM, by United States Department of Agriculture-ARS CRIS
688 projects 5090-31320-004-00D, 8082-32000-007-00-D, and cooperative agreement #5090-31320-
689 004-03S. The views contained in this document are those of the authors and should not be
690 interpreted as necessarily representing the official policies, either expressed or implied, of the
691 U.S. Government. Mention of trade name, proprietary product, or specific equipment does not
692 constitute a guarantee or warranty by the USDA and does not imply its approval to the exclusion
693 of other products that may be suitable. This manuscript is submitted for publication with the
694 understanding that the United States Government is authorized to reproduce and distribute
695 reprints for governmental purposes. The USDA is an equal opportunity employer.

696
697 **References**
698
699 1. Dalsgaard I. 1993. Virulence mechanisms in *Cytophaga psychrophila* and other
700 *Cytophaga*-like bacteria pathogenic for fish. Annu Rev Fish Dis:127-144.
701 2. Nematollahi A, Decostere A, Pasmans F, Haesebrouck F. 2003. *Flavobacterium*
702 *psychrophilum* infections in salmonid fish. J Fish Dis 26:563-574.
703 3. Starliper CE. 2011. Bacterial coldwater disease of fishes caused by
704 *Flavobacterium psychrophilum*. Journal of Advanced Research 2:97-108.
705 4. Miwa S, Nakayasu C. 2005. Pathogenesis of experimentally induced bacterial
706 cold water disease in ayu *Plecoglossus altivelis*. Diseases of Aquatic Organisms
707 67:93-104.
708 5. Soares SMC, Walker A, Elwenn SA, Bayliss S, Garden A, Stagg HEB, Munro
709 ES. 2019. First isolation of *Flavobacterium psychrophilum* associated with
710 reports of moribund wild European eel (*Anguilla anguilla*) in Scotland. Journal of
711 Fish Diseases 42:1509-1521.
712 6. Gomez E, Mendez J, Cascales D, Guijarro JA. 2014. *Flavobacterium*
713 *psychrophilum* vaccine development: a difficult task. Microb Biotechnol 7:414-
714 423.
715 7. Sundell K, Landor L, Nicolas P, Jorgensen J, Castillo D, Middelboe M, Dalsgaard
716 I, Donati VL, Madsen L, Wiklund T. 2019. Phenotypic and genetic predictors of
717 pathogenicity and virulence in *Flavobacterium psychrophilum*. Front Microbiol
718 10:1711.
719 8. Christiansen RH, Madsen L, Dalsgaard I, Castillo D, Kalatzis PG, Middelboe M.
720 2016. Effect of bacteriophages on the growth of *Flavobacterium psychrophilum*
721 and development of phage-resistant strains. Microb Ecol 71:845-59.
722 9. Evenhuis JP, Leeds TD, Marancik DP, LaPatra SE, Wiens GD. 2015. Rainbow
723 trout (*Oncorhynchus mykiss*) resistance to columnaris disease is heritable and
724 favorably correlated with bacterial cold water disease resistance. Journal of
725 animal science 93:1546-54.
726 10. Wiens GD, Palti Y, Leeds TD. 2018. Three generations of selective breeding
727 improved rainbow trout (*Oncorhynchus mykiss*) disease resistance against
728 natural challenge with *Flavobacterium psychrophilum* during early life-stage
729 rearing. Aquaculture 497:414-421.
730 11. Silva RMO, Evenhuis JP, Vallejo RL, Tsuruta S, Wiens GD, Martin KE, Parsons
731 JE, Palti Y, Lourenco DAL, Leeds TD. 2019. Variance and covariance estimates
732 for resistance to bacterial cold water disease and columnaris disease in two
733 rainbow trout breeding populations. Journal of Animal Science 97:1124-1132.
734 12. Duchaud E, Boussaha M, Loux V, Bernardet JF, Michel C, Kerouault B, Mondot
735 S, Nicolas P, Bossy R, Caron C, Bessières P, Gibrat JF, Claverol S, Dumetz F,
736 Hénaff ML, Benmansour A. 2007. Complete genome sequence of the fish
737 pathogen *Flavobacterium psychrophilum*. Nat Biotechnol 25:763-769.
738 13. Wu AK, Kropinski AM, Lumsden JS, Dixon B, MacInnes JI. 2015. Complete
739 genome sequence of the fish pathogen *Flavobacterium psychrophilum* ATCC
740 49418(T.). Stand Genomic Sci 10:3.

14. Pérez-Pascual D, Rochat T, Kerouault B, Gomez E, Neulat-Ripoll F, Henry C, Quillet E, Guijarro JA, Bernardet JF, Duchaud E. 2017. More than gliding: Involvement of GldD and GldG in the virulence of *Flavobacterium psychrophilum*. Frontiers in Microbiology 8.
15. Castillo D, Christiansen RH, Dalsgaard I, Madsen L, Espejo R, Middelboe M. 2016. Comparative genome analysis provides insights into the pathogenicity of *Flavobacterium psychrophilum*. PLoS One 11:e0152515.
16. McBride MJ, Zhu Y. 2013. Gliding motility and Por secretion system genes are widespread among members of the phylum *Bacteroidetes*. J Bacteriol 195:270-278.
17. Sato K, Naito M, Yukitake H, Hirakawa H, Shoji M, McBride MJ, Rhodes RG, Nakayama K. 2010. A protein secretion system linked to bacteroidete gliding motility and pathogenesis. Proc Natl Acad Sci USA 107:276-281.
18. McBride MJ. 2019. Bacteroidetes gliding motility and the type IX secretion system. Microbiol Spectr 7:PSIB-0002-2018.
19. Veith PD, Glew MD, Gorasia DG, Reynolds EC. 2017. Type IX secretion: the generation of bacterial cell surface coatings involved in virulence, gliding motility and the degradation of complex biopolymers. Mol Microbiol 106:35-53.
20. Lasica AM, Ksiazek M, Madej M, Potempa J. 2017. The type IX secretion system (T9SS): Highlights and recent insights into its structure and function. Front Cell Infect Microbiol 7:215.
21. Li N, Zhu Y, LaFrentz BR, Evenhuis JP, Hunnicutt DW, Conrad RA, Barbier P, Gullstrand CW, Roets JE, Powers JL, Kulkarni SS, Erbes DH, Garcia JC, Nie P, McBride MJ. 2017. The type IX secretion system is required for virulence of the fish pathogen *Flavobacterium columnare*. Appl Environ Microbiol 83:e01769-17.
22. Shrivastava A, Johnston JJ, van Baaren JM, McBride MJ. 2013. *Flavobacterium johnsoniae* GldK, GldL, GldM, and SprA are required for secretion of the cell surface gliding motility adhesins SprB and RemA. Journal of bacteriology 195:3201-12.
23. Johnston JJ, Shrivastava A, McBride MJ. 2018. Untangling *Flavobacterium johnsoniae* gliding motility and protein secretion. J Bacteriol 200.
24. Nakane D, Sato K, Wada H, McBride MJ, Nakayama K. 2013. Helical flow of surface protein required for bacterial gliding motility. Proc Natl Acad Sci USA 110:11145-11150.
25. Lauber F, Deme JC, Lea SM, Berks BC. 2018. Type 9 secretion system structures reveal a new protein transport mechanism. Nature 564:77-82.
26. Gorasia DG, Veith PD, Hanssen EG, Glew MD, Sato K, Yukitake H, Nakayama K, Reynolds EC. 2016. Structural insights into the PorK and PorN components of the *Porphyromonas gingivalis* type IX secretion system. PLoS Pathog 12:e1005820.
27. Vincent MS, Canestrari MJ, Leone P, Stathopulos J, Ize B, Zoued A, Cambillau C, Kellenberger C, Roussel A, Cascales E. 2017. Characterization of the *Porphyromonas gingivalis* type IX secretion trans-envelope PorKLMNP core complex. J Biol Chem 292:3252-3261.
28. Leone P, Roche J, Vincent MS, Tran QH, Desmyter A, Cascales E, Kellenberger C, Cambillau C, Roussel A. 2018. Type IX secretion system PorM and gliding

machinery GldM form arches spanning the periplasmic space. Nature Communications 9:ARTN 429.
29. Glew MD, Veith PD, Chen D, Seers CA, Chen YY, Reynolds EC. 2014. Blue native-PAGE analysis of membrane protein complexes in *Porphyromonas gingivalis*. J Proteomics 110:72-92.
30. Kulkarni SS, Johnston JJ, Zhu Y, Hying ZT, McBride MJ. 2019. The carboxy-terminal region of *Flavobacterium johnsoniae* SprB facilitates its secretion by the type IX secretion system and propulsion by the gliding motility machinery. J Bacteriol 201:e00218-19.
31. Kulkarni SS, Zhu Y, Brendel CJ, McBride MJ. 2017. Diverse C-terminal sequences involved in *Flavobacterium johnsoniae* protein secretion. J Bacteriol 199:e00884-16.
32. Glew MD, Veith PD, Peng B, Chen YY, Gorasia DG, Yang Q, Slakeski N, Chen D, Moore C, Crawford S, Reynolds E. 2012. PG0026 is the C-terminal signal peptidase of a novel secretion system of *Porphyromonas gingivalis*. J Biol Chem 287:24605-24617.
33. Kharade SS, McBride MJ. 2014. *Flavobacterium johnsoniae* chitinase ChiA is required for chitin utilization and is secreted by the type IX secretion system. Journal of bacteriology 196:961-70.
34. Veith PD, Muhammad NAN, Dashper SG, Likic VA, Gorasia DG, Chen D, Byrne SJ, Catmull DV, Reynolds EC. 2013. Protein substrates of a novel secretion system are numerous in the *Bacteroidetes* phylum and have in common a cleavable C-terminal secretion signal, extensive post-translational modification, and cell-surface attachment. Journal of Proteome Research 12:4449-4461.
35. Gorasia DG, Veith PD, Chen D, Seers CA, Mitchell HA, Chen YY, Glew MD, Dashper SG, Reynolds EC. 2015. *Porphyromonas gingivalis* type IX secretion substrates are cleaved and modified by a sortase-like mechanism. PLoS Pathog 11:e1005152.
36. Kharade SS, McBride MJ. 2015. *Flavobacterium johnsoniae* PorV is required for secretion of a subset of proteins targeted to the type IX secretion system. J Bacteriol 197:147-158.
37. Sato K, Yukitake H, Narita Y, Shoji M, Naito M, Nakayama K. 2013. Identification of *Porphyromonas gingivalis* proteins secreted by the Por secretion system. FEMS microbiology letters 338:68-76.
38. Kondo Y, Sato K, Nagano K, Nishiguchi M, Hoshino T, Fujiwara T, Nakayama K. 2018. Involvement of PorK, a component of the type IX secretion system, in *Prevotella melaninogenica* pathogenicity. Microbiol Immunol 62:554-566.
39. Chen Z, Wang X, Ren X, Han W, Malhi KK, Ding C, Yu S. 2019. *Riemerella anatipestifer* GldM is required for bacterial gliding motility, protein secretion, and virulence. Vet Res 50:43.
40. Malhi KK, Wang X, Chen Z, Ding C, Yu S. 2019. *Riemerella anatipestifer* gene AS87_08785 encodes a functional component, GldK, of the type IX secretion system. Vet Microbiol 231:93-99.
41. Guo Y, Hu D, Guo J, Wang T, Xiao Y, Wang X, Li S, Liu M, Li Z, Bi D, Zhou Z. 2017. *Riemerella anatipestifer* type IX secretion system is required for virulence and gelatinase secretion. Front Microbiol 8:2553.

42. Alvarez B, Secades P, McBride MJ, Guijarro JA. 2004. Development of genetic techniques for the psychrotrophic fish pathogen *Flavobacterium psychrophilum*. Appl Environ Microbiol 70:581-587.
43. Gomez E, Alvarez B, Duchaud E, Guijarro JA. 2015. Development of a markerless deletion system for the fish-pathogenic bacterium *Flavobacterium psychrophilum*. PLOS One 10:e0117969.
44. Li N, Qin T, Zhang XL, Huang B, Liu ZX, Xie HX, Zhang J, McBride MJ, Nie P. 2015. Gene deletion strategy to examine the involvement of the two chondroitin lyases in *Flavobacterium columnare* virulence. Applied and environmental microbiology 81:7394-402.
45. Zhu Y, Thomas F, Larocque R, Li N, Duffieux D, Cladiere L, Souchaud F, Michel G, McBride MJ. 2017. Genetic analyses unravel the crucial role of a horizontally acquired alginate lyase for brown algal biomass degradation by *Zobellia galactanivorans*. Environ Microbiol 19:2164-2181.
46. Link AJ, Phillips D, Church GM. 1997. Methods for generating precise deletions and insertions in the genome of wild-type *Escherichia coli*: application to open reading frame characterization. J Bacteriol 179:6228-6237.
47. Rochat T, Barbier P, Nicolas P, Loux V, Pérez-Pascual D, Guijarro JA, Bernardet J-F, Duchaud E. 2017. Complete genome sequence of *Flavobacterium psychrophilum* strain OSU THCO2-90. Genome Announc 5.
48. Ikegami A, Honma K, Sharma A, Kuramitsu HK. 2004. Multiple functions of the leucine-rich repeat protein LrrA of *Treponema denticola*. Infect Immun 72:4619-27.
49. Sharma A, Sojar HT, Glurich I, Honma K, Kuramitsu HK, Genco RJ. 1998. Cloning, expression, and sequencing of a cell surface antigen containing a leucine-rich repeat motif from *Bacteroides forsythus* ATCC 43037. Infect Immun 66:5703-10.
50. Nelson SS, Bollampalli S, McBride MJ. 2008. SprB is a cell surface component of the *Flavobacterium johnsoniae* gliding motility machinery. J Bacteriol 190:2851-2857.
51. Wiens GD, LaPatra SE, Welch TJ, Rexroad C, 3rd, Call DR, Cain KD, LaFrentz BR, Vaisvil B, Schmitt DP, Kapatral V. 2014. Complete genome sequence of *Flavobacterium psychrophilum* strain CSF259-93, used to select rainbow trout for increased genetic resistance against bacterial cold water disease. Genome Announc 2.
52. Rhodes RG, Nelson SS, Pochiraju S, McBride MJ. 2011. *Flavobacterium johnsoniae sprB* is part of an operon spanning the additional gliding motility genes *sprC*, *sprD*, and *sprF*. J Bacteriol 193:599-610.
53. Heath JE, Seers CA, Veith PD, Butler CA, Nor Muhammad NA, Chen YY, Slakeski N, Peng B, Zhang L, Dashper SG, Cross KJ, Cleal SM, Moore C, Reynolds EC. 2016. PG1058 is a novel multidomain protein component of the bacterial type IX secretion system. PLoS One 11:e0164313.
54. Ortiz-Suarez ML, Samsudin F, Piggot TJ, Bond PJ, Khalid S. 2016. Full-length OmpA: structure, function, and membrane interactions predicted by molecular dynamics simulations. Biophysical Journal 111:1692-1702.

55. Samsudin F, Ortiz-Suarez ML, Piggot TJ, Bond PJ, Khalid S. 2016. OmpA: a flexible clamp for bacterial cell wall attachment. Structure 24:2227-2235.
56. Rhodes RG, Samarasam MN, Shrivastava A, van Baaren JM, Pochiraju S, Bollampalli S, McBride MJ. 2010. *Flavobacterium johnsoniae gldN* and *gldO* are partially redundant genes required for gliding motility and surface localization of SprB. J Bacteriol 192:1201-1211.
57. Braun TF, Khubbar MK, Saffarini DA, McBride MJ. 2005. *Flavobacterium johnsoniae* gliding motility genes identified by *mariner* mutagenesis. J Bacteriol 187:6943-6952.
58. Zhu Y, McBride MJ. 2016. Comparative analysis of *Cellulophaga algicola* and *Flavobacterium johnsoniae* gliding motility. J Bacteriol 198:1743-54.
59. Pérez-Pascual D, Menendez A, Fernandez L, Mendez J, Reimundo P, Navais R, Guijarro JA. 2009. Spreading versus biomass production by colonies of the fish pathogen *Flavobacterium psychrophilum*: role of the nutrient concentration. Int Microbiol 12:207-14.
60. Bernardet JF, Kerouault B. 1989. Phenotypic and genomic studies of "*Cytophaga psychrophila*" isolated from diseased rainbow trout (*Oncorhynchus mykiss*) in France. Appl Environ Microbiol 55:1796-1800.
61. Holt RA, Amandi A, Rohovec J, Fryer J. 1988. Relation of water temperature to *Cytophaga psychrophila* infection in coho (*Oncorhynchus kisutch*) and chinook salmon (*O. tshawytscha*) and rainbow trout (*Salmo gairdneri*). *In* Society AF (ed), International Fish Health Conference Handbook. International Fish Health Conference, Vancouver, Canada.
62. Pishchany G, Skaar EP. 2012. Taste for blood: hemoglobin as a nutrient source for pathogens. PLoS Pathog 8:e1002535.
63. Högfors-Rönnholm E, Wiklund T. 2010. Hemolytic activity in *Flavobacterium psychrophilum* is a contact-dependent, two-step mechanism and differently expressed in smooth and rough phenotypes. Microbial Pathogenesis 49:369-375.
64. Moller JD, Ellis AE, Barnes AC, Dalsgaard I. 2005. Iron acquisition mechanisms of *Flavobacterium psychrophilum*. Journal of Fish Diseases 28:391-398.
65. Nakayama K. 2015. *Porphyromonas gingivalis* and related bacteria: from colonial pigmentation to the type IX secretion system and gliding motility. Journal of Periodontal Research 50:1-8.
66. Halpern D, Gruss A. 2015. A sensitive bacterial-growth-based test reveals how intestinal *Bacteroides* meet their porphyrin requirement. Bmc Microbiology 15.
67. Hogfors-Ronnholm E, Norrgard J, Wiklund T. 2015. Adhesion of smooth and rough phenotypes of *Flavobacterium psychrophilum* to polystyrene surfaces. Journal of Fish Diseases 38:429-437.
68. Alvarez B, Secades P, Prieto M, McBride MJ, Guijarro JA. 2006. A mutation in *Flavobacterium psychrophilum tlpB* inhibits gliding motility and induces biofilm formation. Appl Environ Microbiol 72:4044-4053.
69. Sundell K, Wiklund T. 2011. Effect of biofilm formation on antimicrobial tolerance of *Flavobacterium psychrophilum*. Journal of Fish Diseases 34:373-383.
70. Hadidi S, Glenney GW, Welch TJ, Silverstein JT, Wiens GD. 2008. Spleen size predicts resistance of rainbow trout to *Flavobacterium psychrophilum* challenge. Journal of Immunology 180:4156-4165.

71. Levipan HA, Avendano-Herrera R. 2017. Different phenotypes of mature biofilm in *Flavobacterium psychrophilum* share a potential for virulence that differs from planktonic state. Front Cell Infect Microbiol 7:76.
72. Braun TF, McBride MJ. 2005. *Flavobacterium johnsoniae* GldJ is a lipoprotein that is required for gliding motility. J Bacteriol 187:2628-2637.
73. LaFrentz BR, LaPatra SE, Call DR, Cain KD. 2008. Isolation of rifampicin resistant *Flavobacterium psychrophilum* strains and their potential as live attenuated vaccine candidates. Vaccine 26:5582-9.
74. Gliniewicz K, Wildung M, Orfe LH, Wiens GD, Cain KD, Lahmers KK, Snekvik KR, Call DR. 2015. Potential mechanisms of attenuation for rifampicin-passaged strains of *Flavobacterium psychrophilum*. BMC Microbiol 15:179.
75. Bertolini JM, Wakabayashi H, Watral VG, Whipple MJ, Rohovec JS. 1994. Electrophoretic detection of proteases from selected strains of *Flexibacter psychrophilus* and assessment of their variability. J Aquat Anim Health 6:224-233.
76. Cain KD, LaFrentz BR. 2007. Laboratory maintenance of *Flavobacterium psychrophilum* and *Flavobacterium columnare*. Current Protocols in Microbiology 6:13B.1.1-13B.1.12.
77. Holt RA, Rohovec JS, Fryer JL. 1993. Bacterial coldwater disease, p 3-23. *In* Inglis V, Roberts RJ, Bromage NR (ed), Bacterial diseases of fish. Blackwell Scientific Publications, Oxford.
78. Cato EP, Johnson JL. 1976. Reinstatement of species rank for *Bacteroides fragilis*, *B. ovatus*, *B. distasonis*, *B. thetaiotaomicron*, and *B. vulgatus*: Designation of neotype strains for *Bacteroides fragilis* (Veillon and Zuber) Castellani and Chalmers and *Bacteroides thetaiotaomicron* (Distaso) Castellani and Chalmers. Int J Syst Bacteriol 26:230-237.
79. Bertani G. 1951. Studies on lysogenesis I. The mode of phage liberation by lysogenic *Escherichia coli*. J Bacteriol 62:293-300.
80. McBride MJ, Kempf MJ. 1996. Development of techniques for the genetic manipulation of the gliding bacterium *Cytophaga johnsonae*. J Bacteriol 178:583-590.
81. Laemmli UK. 1970. Cleavage of structural proteins during the assembly of the head of bacteriophage T4. Nature 227:680-5.
82. Newton JC, Wood TM, Hartley MM. 1997. Isolation and partial characterization of extracellular proteases produced by isolates of *Flavobacterium columnare* derived from catfish. Journal of aquatic animal health 9:75-85.
83. Wiens GD, LaPatra SE, Welch TJ, Evenhuis JP, Rexroad CE, Leeds TD. 2013. On-farm performance of rainbow trout (*Oncorhynchus mykiss*) selectively bred for resistance to bacterial cold water disease: Effect of rearing environment on survival phenotype. Aquaculture 388:128-136.
84. Quillet E, Dorson M, Le Guillou S, Benmansour A, Boudinot P. 2007. Wide range of susceptibility to rhabdoviruses in homozygous clones of rainbow trout. Fish & Shellfish Immunology 22:510-519.
85. Fraslin C, Dechamp N, Bernard M, Krieg F, Hervet C, Guyomard R, Esquerre D, Barbieri J, Kuchly C, Duchaud E, Boudinot P, Rochat T, Bernardet JF, Quillet E. 2018. Quantitative trait loci for resistance to *Flavobacterium psychrophilum* in

rainbow trout: effect of the mode of infection and evidence of epistatic interactions. Genet Sel Evol 50:60.

86. Haft DH, Selengut JD, Richter RA, Harkins D, Basu MK, Beck E. 2013. TIGRFAMs and genome properties in 2013. Nucleic Acids Res 41:D387-95.

87. de Lorenzo V, Timmis KN. 1994. Analysis and construction of stable phenotypes in gram-negative bacteria with Tn5- and Tn10-derived minitransposons. Methods in enzymology 235:386-405.

979 **Table 1. Predicted T9SS type A CTD-containing proteins of *F. psychrophilum* strain OSU THCO2-90[1]**
980

Locus tag	Protein name	AA[2]	Mol. Mass (kDa)[3]	Domains[4]	Description/ known or predicted function
THC0290_0086		642	70.9	M1_APN_like (cd09603) Peptidase_M1 (pfam01433)	Probable peptidase precursor (M1 family metalloprotease)
THC0290_0091		1139	122.8	Sortilin-Vps10 super family (cl25791) Peptidase_M6 super family (cl29544)	Probable glycoside hydrolase precursor
THC0290_0128		113	12.8		
THC0290_0129		324	33.6		Putative outer membrane protein precursor
THC0290_0170		398	41.7	LRR_5 (pfam13306)	Probable cell surface protein (Leucine-rich repeat protein) precursor
THC0290_0171		421	44.5	LRR_5 (pfam13306)	Probable cell surface protein precursor (Leucine-rich repeat protein) precursor
THC0290_0172		329	35.2	LRR_5 (pfam13306)	Probable cell surface protein (Leucine-rich repeat protein)
THC0290_0173		444	47.2	LRR_5 (pfam13306)	Probable cell surface protein (Leucine-rich repeat protein) precursor
THC0290_0174		422	44.5	LRR_5 (pfam13306)	Probable cell surface protein (Leucine-rich repeat protein) precursor
THC0290_0175		330	35.3	LRR_5 (pfam13306)	Probable cell surface protein (Leucine-rich repeat protein) precursor
THC0290_0176		375	40.1	LRR_5 (pfam13306)	Probable cell surface protein (Leucine-rich repeat protein) precursor
THC0290_0177		536	56.0	LRR_5 (pfam13306)	Probable cell surface protein (Leucine-rich repeat protein) precursor
THC0290_0178		307	33.1	LRR_5 (pfam13306)	Probable cell surface protein (Leucine-rich repeat protein) precursor
THC0290_0179		421	44.3	LRR_5 (pfam13306)	Probable cell surface protein (Leucine-rich repeat protein) precursor
THC0290_0180		398	42.1	LRR_5 (pfam13306)	Probable cell surface protein (Leucine-rich repeat protein) precursor
THC0290_0181		467	50.1	LRR_5 (pfam13306)	Probable cell surface protein (Leucine-rich repeat protein) precursor
THC0290_0182		329	35.0	LRR_5 (pfam13306)	Probable cell surface protein (Leucine-rich repeat protein) precursor
THC0290_0183		306	33.2	LRR_5 (pfam13306)	Probable cell surface protein (Leucine-rich repeat protein) precursor
THC0290_0184		351	37.0	LRR_5 (pfam13306)	Probable cell surface protein (Leucine-rich repeat protein)

					precursor
THC0290_0185		329	35.3	LRR_5 (pfam13306)	Probable cell surface protein (Leucine-rich repeat protein) precursor
THC0290_0186		328	35.3	LRR_5 (pfam13306)	Probable cell surface protein (Leucine-rich repeat protein) precursor
THC0290_0237	Fpp1	1138	119.6	ZnMc super family (cl00064) FN3 super family (cl21522) P_proprotein super family (cl27557)	Peptidase precursor (Psychrophilic metalloprotease Fpp1)
THC0290_0238	Fpp2	942	100.3	ZnMc_pappalysin_like (cd04275) Cleaved_Adhesin super family (cl06636)	Peptidase precursor (Psychrophilic metalloprotease Fpp2)
THC0290_0299		914	100.1	Peptidase_M36 (pfam02128) PA_subtilisin_1 (cd04818)	Probable peptidase precursor (M36 fungalysin family metalloprotease)
THC0290_0300		919	99.8	Peptidase_M36 (pfam02128) PA_subtilisin_1 (cd04818)	Probable peptidase precursor (M36 fungalysin family metalloprotease)
THC0290_0878		747	78.2	FN3 (cd00063)	Putative adhesin precursor
THC0290_0931		960	103.3	ZnMc super family (cl00064)	Peptidase precursor (Collagenase; Zn-dependent metalloprotease)
THC0290_0944		544	58.5	Peptidases_S8_9 (cd07493)	Probable peptidase precursor (S8 subtilisin family serine endopeptidase)
THC0290_0977		585	64.9	Abhydrolase super family (cl21494)	Esterase/lipase/thioesterase family protein precursor
THC0290_1054		408	46.0	SGNH_hydrolase super family (cl01053) PKD repeat (COG3291)	
THC0290_1343		1218	134.1	ZnMc super family (cl00064) PKD (COG3291, 3 copies) PCC super family (cl28216)	Probable cell surface protein precursor; putative metallopeptidase, metzincin clan
THC0290_1494		657	71.5	HNHc super family (cl00083)	Probable ribonuclease
THC0290_1520		613	66.2	Endonuclease_1 (pfam04231) FN3 (cd00063) COG2374 super family (cl28586)	Probable endonuclease precursor
THC0290_1595		628	67.9		Putative adhesin precursor
THC0290_1797		263	29.4	DOMON_DOH (cd09631)	
THC0290_2029		301	32.9		
THC0290_2146	PorU	1278	142.1	Peptidase_C25_N (cd02258)	Peptidase precursor (T9SS CTD signal peptidase, PorU)
THC0290_2157		166	18.7		
THC0290_2385		456	49.2	ATS1 super family (cl34932) RCC1 (pfam00415)	RCC1 (Regulator of Chromosome Condensation) repeat domain protein precursor
Average		550	59.3		
Median		422	46.0		

Range	113 to 1278	12.8 to 142.1

[1]The T9SS type A CTD (TIGR04183) is a C-terminal domain that targets a protein for secretion by the T9SS. TIGR04183 is described as 'Por secretion system C-terminal sorting domain' on the J. Craig Venter Institute TIGR website (http://www.jcvi.org/cgi-bin/tigrfams/index.cgi). Each of these proteins contains an N-terminal signal peptide for export across the cytoplasmic membrane as determined using SignalP 5.0 with a cutoff of 0.8, and a T9SS type A C-terminal domain (CTD) for secretion across the outer membrane by the T9SS as determined using the Integrated Microbial Genomes (IMG version 4.0.1 [https://img.jgi.doe.gov/]) tools and trusted cutoffs.

[2]Length of full-length protein in amino acids before removal of signal peptide or CTD.

[3]Molecular mass (kDa) of full-length protein in amino acids before removal of signal peptide or CTD.

[4]Domains other than signal peptide and CTDs, with pfam, cl, cd, or COG numbers indicated.

994 **Table 2. Predicted T9SS type B CTD-containing proteins of *F. psychrophilum* strain OSU THCO2-90[1]**
995

Locus tag	Name	AA[2]	Mol. Mass (kDa)[3]	Domains[4]	Description/Function or predicted function
THC0290_0023	SprC	477	51.2	FlgD_ig super family (cl21544)	Gliding motility protein precursor, SprC
THC0290_0025	SprB	3521	366.8	SprB repeat (pfam13573, 3 copies) FlgD Ig-like domain (cl21544)	Gliding motility adhesin precursor, SprB
THC0290_0332		2653	269.2	ATS1 super family (cl34932) Calx-beta domain (cl02522) Herpes_BLLF1 super family (cl37540)	Putative adhesin precursor
THC0290_1047		798	87.8		Putative adhesin precursor
THC0290_1048		757	82.6		Putative adhesin precursor
THC0290_1527		2229	233.6	Ig_2 (pfam13895)	Putative adhesin precursor
THC0290_1616		1253	129.6	YjdB (COG5492, 2 copies) Big_2 (cl02708)	Putative adhesin precursor
THC0290_1818		1452	158.9		Putative adhesin precursor
THC0290_1932		2001	200.0	DUF11 (pfam01345) PRK08026 super family (cl35635)	Putative adhesin precursor
THC0290_2338		2008	208.3	fn3 (pfam00041, 2 copies) FN3 (cd00063, 2 copies) CUB (cd00041)	Putative adhesin precursor
Average		1715	178.8		
Median		1727	179.5		
Range		477 to 3521	51.2 to 366.8		

996
997 [1]The T9SS type B CTD (TIGR04131/pfam13585) is a C-terminal domain that targets a protein for secretion by the T9SS. TIGR04131
998 is described as 'gliding motility-associated C-terminal domain' on the J. Craig Venter Institute TIGR website (http://www.jcvi.org/cgi-
999 bin/tigrfams/index.cgi). Each of these proteins contains an N-terminal signal peptide for export across the cytoplasmic membrane as
1000 determined using SignalP 5.0 with a cutoff of 0.7, and a T9SS type B CTD for secretion across the outer membrane by the T9SS as
1001 determined using the IMG tools and trusted cutoffs. THC0290_0023 (SprC) matched only pfam13585, whereas each of the other
1002 proteins matched both TIGR04131 and pfam13585.
1003

[2]Length of full-length protein in amino acids before removal of signal peptide or CTD.

[3]Molecular mass (kDa) of full-length protein in amino acids before removal of signal peptide or CTD.

[4]Domains other than signal peptide and CTDs, with pfam, cl, cd, or COG numbers indicated.

1010 **Table 3. *F. psychrophilum* T9SS type A CTD and type B CTD proteins identified by LC-MS/MS analysis of cell-free spent**

1011 **culture medium**[a]

1012

Locus tag/Protein name	Mol. Mass (kDa) [b]	T9SS CTD[c]	Predicted protein function or description	Spectral counts from culture fluid		
				Wild type	Δ*gldN*	Δ*gldN* + pBFp4
T9SS-CTD proteins other than leucine-rich repeat proteins						
THC0290_0238 /Fpp2	100.3	type A	Peptidase	813	72	903
THC0290_0025 /SprB	366.8	type B	Gliding motility adhesin SprB	268	59	315
THC0290_0931	103.3	type A	Peptidase (collagenase)	170	22	143
THC0290_2338	208.3	type B	Adhesin	84	32	94
THC0290_1932	200.0	type B	Adhesin	48	17	36
THC0290_1520	66.2	type A	Endonuclease	37	0	40
THC0290_2029	32.9	type A		34	19	45
THC0290_1797	29.4	type A		32	1	23
THC0290_1616	129.6	type B	Adhesin	27	8	53
THC0290_1595	67.9	type A	Adhesin	24	8	16

THC0290_0944	58.5	type A	Peptidase	21	0	23
THC0290_2146	142.1	type A	T9SS-specific CTD peptidase	20	17	32
/PorU						
THC0290_1494	71.5	type A	Ribonuclease	19	0	24
THC0290_0332	269.2	type B	Adhesin	15	4	16
THC0290_1527	233.6	type B	Adhesin	13	5	20
THC0290_0023	51.2	type B	Gliding motility protein SprC	9	4	9
/SprC						
THC0290_1047	87.8	type B	Adhesin	8	1	15
THC0290_1343	134.1	type A	Peptidase	6	0	6
THC0290_0086	70.9	type A	Peptidase	6	0	9
THC0290_0237	119.6	type A	Peptidase	6	0	5
/Fpp1						
THC0290_0129	33.6	type A		6	1	9
THC0290_1818	158.9	type B	Adhesin	6	0	6
THC0290_0091	122.8	type A	Glycoside hydrolase	5	2	4
THC0290_1048	82.6	type B	Adhesin	3	0	7
THC0290_0299	100.1	type A	Peptidase	1	16	6
THC0290_1054	46.0	type A		0	0	3
THC0290_0128	12.8	type A		0	2	0

Leucine-rich repeat proteins[d]						
THC0290_0183	33.2	type A	leucine-rich repeat protein	51	22	46
THC0290_0174	44.5	type A	leucine-rich repeat protein	23	13	22
THC0290_0171	44.5	type A	leucine-rich repeat protein	22	18	32
THC0290_0170	41.7	type A	leucine-rich repeat protein	20	40	24
THC0290_0181	50.1	type A	leucine-rich repeat protein	17	18	18
THC0290_0184	37.0	type A	leucine-rich repeat protein	15	25	23
THC0290_0186	35.3	type A	leucine-rich repeat protein	12	15	13
THC0290_0182	35.0	type A	leucine-rich repeat protein	9	17	10
THC0290_0175	35.3	type A	leucine-rich repeat protein	7	16	12
THC0290_0185	35.3	type A	leucine-rich repeat protein	7	9	10
THC0290_0172	35.2	type A	leucine-rich repeat protein	7	19	11
THC0290_0180	42.1	type A	leucine-rich repeat protein	0	20	0
THC0290_0177	56.0	type A	leucine-rich repeat protein	0	15	0

[a] Proteins in cell-free culture fluid from wild-type *F. psychrophilum*, Δ*gldN* mutant, and Δ*gldN* complemented with pBFp4, were analyzed by LC-MS/MS. Total/unweighted spectrum counts corresponding to total number of spectra associated to a single protein and indicative of relative abundance of that protein are indicated for each strain. Only proteins with predicted T9SS CTDs are shown. For the full dataset, which includes additional proteins, see Dataset S1. The following type A CTD proteins were not detected: THC0290_0173, THC0290_0176, THC0290_0178, THC0290_0179, THC0290_0300, THC0290_0878, THC0290_0977, THC0290_2157, THC0290_2385. However, the LRR proteins THC0290_0173, THC0290_0176, THC0290_0178, THC0290_0179,

may have been present, because they are similar in sequence to the other LRR proteins, resulting in ambiguity regarding protein assignment for some peptides (Dataset S1). Similarly, THC0290_300 may have been missed because of similarity in sequence to THC0290_0299.

[b] Molecular mass as calculated for full-length protein before removal of signal peptide.

[c] Type A CTDs belong to TIGRFAM protein domain family TIGR04183. Type B CTDs belong to TIGRFAM protein domain family TIGR04131 and/or pfam13585.

[d] These proteins have paralogs in the genome that complicate assignment of peptides.

1031 **Table 4. Strains and plasmids used in this study**
1032

Strain or plasmid	Description[a]	Source or reference
Bacteroides thetaiotaomicron strain VPI-5482^T	Used to measure porphyrin (heme, hemoglobin or protoporphyrin IX)	(78)
E. coli DH5αMCR	Strain used for general cloning	Life Technologies (Grand Island, NY)
E. coli S17-1 λ pir	Strain used for conjugation	(87)
F. psychrophilum strain OSU THCO2-90	Wild type	(47, 75)
F. psychrophilum strain FpT13	Δ*gldN* in strain OSU THCO2-90	This study
Plasmids		
pCP11	*E. coli-Flavobacterium* shuttle plasmid; Ap^r (Em)^r	(80)
pYT313	Suicide vector carrying *sacB*; Ap^r (Em^r)	(45)
pBFp0	2,858 bp region upstream of *gldN* amplified with primers 2060 and 2061 and cloned into BamHI and SalI sites of pYT313; Ap^r (Em^r)	This study
pBFp1	Construct used to delete *gldN*; 3,132 bp region downstream of *gldN* amplified with primers 2062 and 2063 and cloned into SalI and SphI sites of pBFp0; Ap^r (Em^r)	This study
pBFp4	Plasmid for complementation of *gldN*; *gldN* was amplified with primers 2076 and 2077 and cloned into KpnI and SphI sites of pCP11; Ap^r (Em^r)	This study

1033

1034 [a]Antibiotic resistance phenotypes: ampicillin, Ap^r; erythromycin, Em^r. Unless indicated

1035 otherwise, the antibiotic resistance phenotypes are those expressed in *E. coli*. The antibiotic

1036 resistance phenotypes given in parentheses are those expressed in *F. psychrophilum* but not in *E.*

1037 *coli*.

1038

1039 **Table 5. Primers used in this study**

Primers	Sequence[a]
2060	5’ GCTAGGGATCCGCTAGAAATGATAGAGGTTGTTATT 3’
2061	5’ GCTAGGTCGACGTCATTATCTTTTAGTTGTTGTGCT 3’
2062	5’ GCTAGGTCGACCGTTTTAATGCACTGACTTATAAAG 3’
2063	5’ GCTAGGCATGCGTAATTTCGCCATCTAGATATTCT 3’
2076	5’ GCTAGGGTACCAGCTAGCTTCTCTGGAATAG 3’
2077	5’ GCTAGGCATGCATTTGGTAAGAGTTTTTTAA 3’

1040

1041 [a]Underlined sequences indicate introduced restriction enzyme sites.

1042

Figure 1. Gliding of wild-type and Δ*gldN* mutant cells on agar

Cells were grown in TYES at 18°C for 24 h to late exponential phase, (OD approximately 1.3). Ten microliters of cultures were spotted on TYES solidified with agar (10 g /l) and observed for motility using an Olympus BH-2 phase-contrast microscope. Wild-type (WT) *F. psychrophilum*, Δ*gldN* mutant, and Δ*gldN* complemented with wild-type *gldN* on pBFp4 are shown. In each case a series of images were taken using a Photometrics Cool-SNAP$_{cf}^2$ camera. Individual frames were colored from red (time 0) to yellow, green, cyan, and finally blue (132 s) and integrated into one image, resulting in 'rainbow traces' of gliding cells. The top row shows the first frame for each strain, and the bottom row shows the corresponding 132 sec rainbow trace. White cells in the bottom panel correspond to cells that exhibited little if any net movement. Bar at lower right (20 μm) applies to all panels. The rainbow traces correspond to the sequences in Movie S1.

Figure 2. Colonies of wild-type, Δ*gldN* mutant, and complemented strains of *F. psychrophilum*

(A-C) Micro-colonies of wild type (WT), Δ*gldN* mutant, and Δ*gldN* mutant complemented with wild-type *gldN* on pBFp4. Colonies arose from cells incubated for 32 h at 18°C on 5% TYES solidified with agar (10 g/l). Photomicrographs were taken with a Photometrics Cool-SNAP$_{cf}^2$ camera mounted on an Olympus IMT-2 phase contrast microscope. Bar in panel C (0.5 mm) applies to panels A, B, and C. (D) Macro-colonies of wild type, Δ*gldN* mutant, and complemented mutant. Cells were spotted on 5% TYES solidified with agar (10 g/l), incubated at 18°C for 12 d, and photographed using a Nikon D7200 camera. Bar in panel D indicates 10 mm.

1067

1068

1069

1070 **Figure 3. Soluble extracellular proteins of wild-type and Δ*gldN* mutant cells**

1071 Cells of wild-type *F. psychrophilum*, Δ*gldN* mutant, and Δ*gldN* mutant complemented with wild-

1072 type *gldN* on pBFp4, were grown in TYES medium at 18°C with shaking until cells reached

1073 early stationary phase of growth (Klett readings of 160). Cells were removed by centrifugation

1074 followed by filtration (0.45 μm). Proteins from equal amounts of cell-free spent media of wild-

1075 type, mutant, and complemented cells were precipitated with TCA, solubilized in loading buffer,

1076 and separated by SDS-PAGE. Proteins were detected by silver staining. Lane labeled 'TYES'

1077 contained an equivalent amount of TYES growth medium that had not been inoculated with *F.*

1078 *psychrophilum*, indicating bands that correspond to components of the growth medium.

Figure 4. Proteolytic activity of wild-type and Δ*gldN* mutant cells

Exoproteolytic activity of *F. psychrophilum* wild type (WT), Δ*gldN* mutant, and Δ*gldN* complemented with pBFp4. A) stationary phase cultures were spotted on TYESG agar supplemented with casein (7.5 g/l) and proteolytic activity was visualized as clearing zones around the bacterial growth after incubation at 18°C for 4 days. B) proteolytic activity measured using azocasein as a substrate. Cells were grown in TYESG broth at 18°C with shaking. Proteolytic activity was measured in cell-free supernatants from each strain at different stages of growth. The results of three experiments are presented (values and error bars are means and standard deviations, respectively). Solid lines: OD_{600} indicating growth. Dashed lines: proteolytic activity units. Color code: blue (WT), red (Δ*gldN*), green (Δ*gldN* complemented with pBFp4).

Figure 5. Hemolytic activity of wild-type and Δ*gldN* mutant cells

Hemolytic activities of cells of *F. psychrophilum* wild type (WT), Δ*gldN* mutant, and Δ*gldN* complemented with pBFp4, incubated for 4 days at 18°C on TYESG agar supplemented with rainbow trout blood (50 ml/l). The results are representative of three independent experiments.

Figure 6. Hemoglobin utilization by wild-type and Δ*gldN* mutant cells

Detection of residual heme after growth of *F. psychrophilum* wild type (WT), Δ*gldN* mutant, and Δ*gldN* complemented with pBFp4 to stationary phase in TYESG broth supplemented with 0.5 µM hemoglobin. The heme-protoporphyrin IX-screen is a bacterial-growth-based assay that exploits *Bacteroides thetaiotaomicron* heme auxotrophy. The stimulation area (cm^2) is proportional to the amount of porphyrin (heme, hemoglobin or protoporphyrin IX) in the sample. TYESG Hb and TYESG Ø: sterile medium with (Hb) or without (Ø) addition of hemoglobin to 0.5 µM. The results correspond to three independent bacterial cultures (mean and standard deviation are presented).

Figure 7. Adhesion, biofilm formation, and sedimentation of wild-type and Δ*gldN* mutant cells

(A) Adhesion of wild-type *F. psychrophilum* (blue), Δ*gldN* mutant (red), and Δ*gldN* mutant complemented with pBFp4 (green) to polystyrene after 3 h of incubation at 18°C without shaking as determined by staining with crystal violet and measuring absorbance at 595 nm. Adhesion shown in relation to the wild-type strain, which was set as 100. (B) Biofilm formation on polystyrene by the same strains (identical color code) grown in half-strength TYES broth for 120 h at 18°C without shaking. (C) Cell sedimentation of the same strains grown in half-strength TYES broth for 96 h at 18°C with shaking at 200 rpm.

1130
1131
1132
1133 **Figure 8. Analysis of virulence of wild-type and Δ*gldN* mutant cells toward rainbow trout**
1134 **following challenge by injection.** Kaplan-Meier survival curves of rainbow trout after
1135 intramuscular injection challenge. Four groups of 20 fish (n=80) were challenged with each *F.*
1136 *psychrophilum* strain at doses (CFU/fish) of 2.6×10^6 (wild type), 2.7×10^6 (Δ*gldN* mutant) and
1137 2.8×10^6 (Δ*gldN* mutant complemented with pBFp4). Survival curves for fish inoculated with
1138 PBS (Control) and for fish inoculated with the Δ*gldN* mutant were identical. Survival curves for
1139 fish inoculated with either the wild type or the Δ*gldN* mutant complemented with pBFp4 are
1140 significantly different from the Δ*gldN* mutant (Mantel-Cox Log-rank test pvalues <0.0001). The
1141 survival curve of the Δ*gldN* mutant complemented with pBFp4 was modestly higher than the
1142 wild type (pvalue = 0.0012).

Figure 9. Analysis of virulence of wild-type and Δ*gldN* mutant cells toward rainbow trout following immersion challenge

Groups of 42 fish were infected by immersion with *F. psychrophilum* wild type (WT), Δ*gldN*, and Δ*gldN* complemented with pBFp4. The results of two independent experiments are presented. A) *F. psychrophilum* bacterial loads in aquarium water during fish infection by immersion. Average of bacterial quantification determined at the beginning (0 h) and end (24 h) of fish infection challenge. B) Kaplan-Meier survival curves of rainbow trout after immersion challenge (each group composed of 30 fish). Survival curves for fish challenged with the Δ*gldN* mutant, or with either the wild type or the Δ*gldN* mutant complemented with pBFp4 are significantly different (Mantel-Cox Log-rank test pvalues <0.0001). Colored shaded areas indicate 95% confidence intervals. C) Bacterial loads in organs of rainbow trout after immersion challenge. Six fish were sacrificed at 6 h and 30 h post-infection for each group. Serial dilutions of homogenized organs were incubated on TYESG agar supplemented with fetal calf serum (50 ml/l) to determine the CFU. Bacterial loads of spleen (left panel) and gills (right panel) are shown. Horizontal dashed line indicates the detection threshold. Values are significantly lower for Δ*gldN* relative to wild-type and complemented strains (Mann-Whitney pvalues < 0.0001).

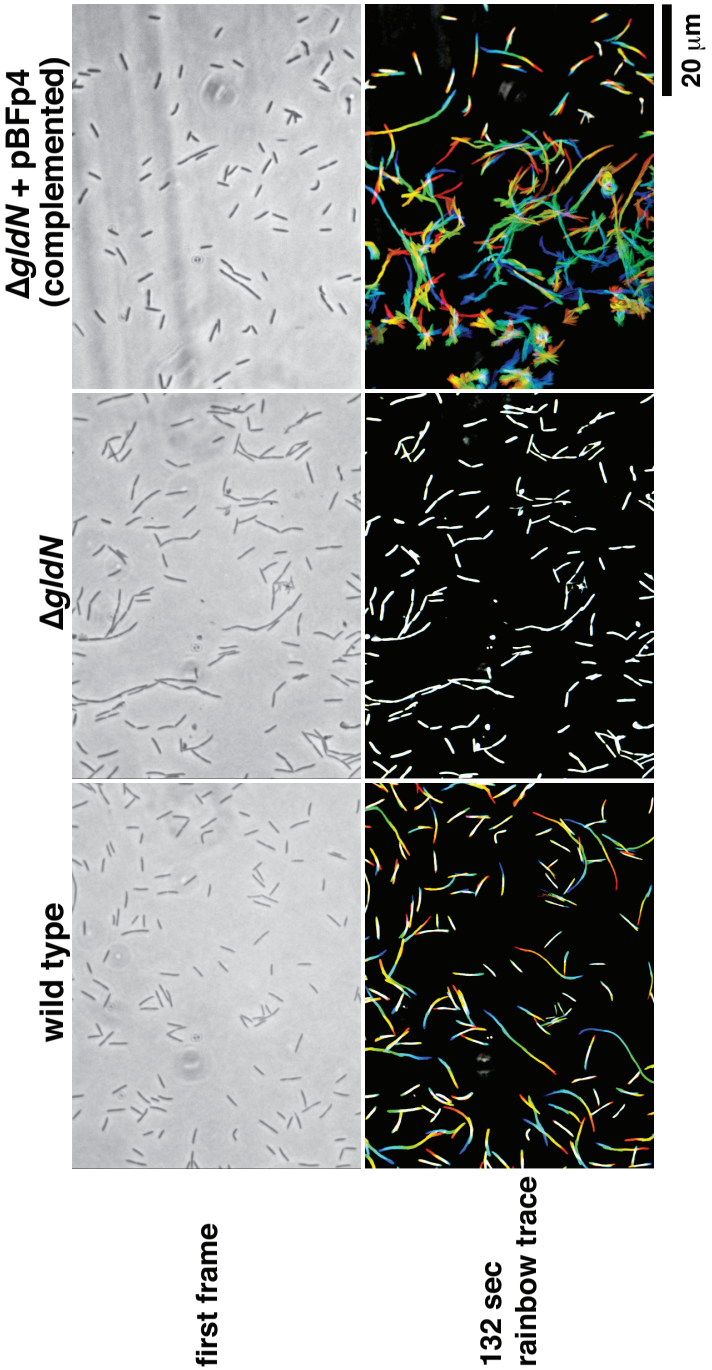

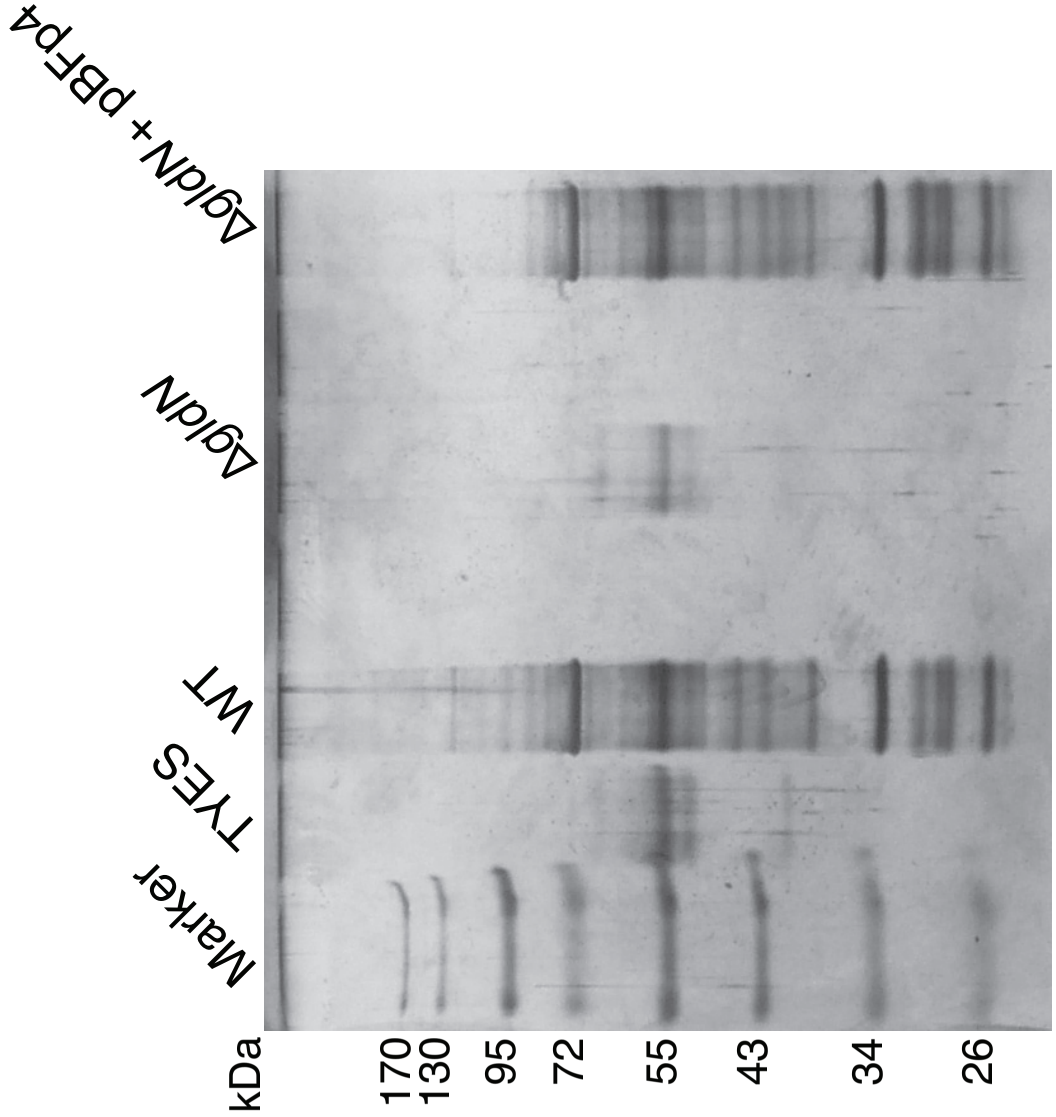

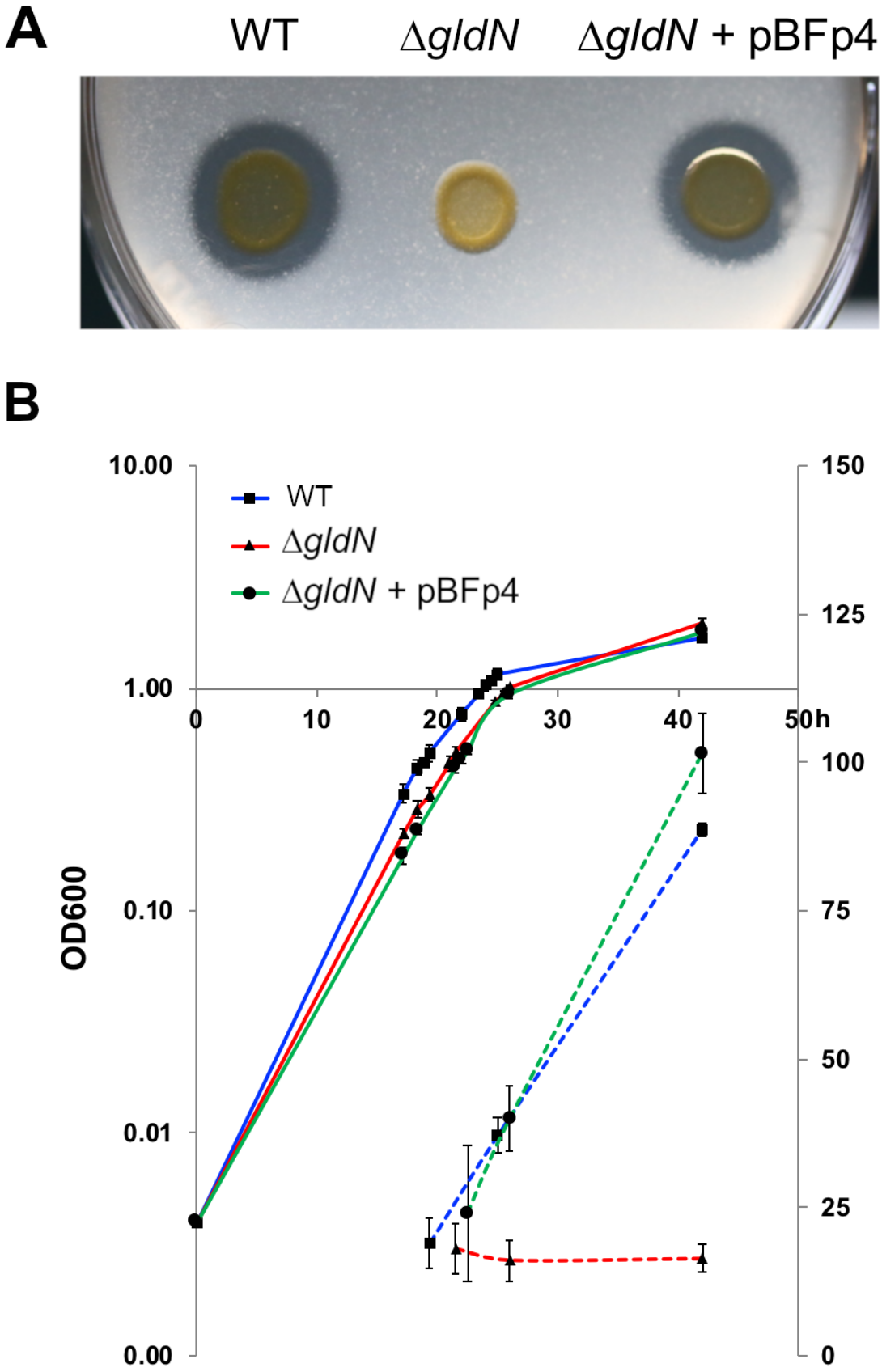

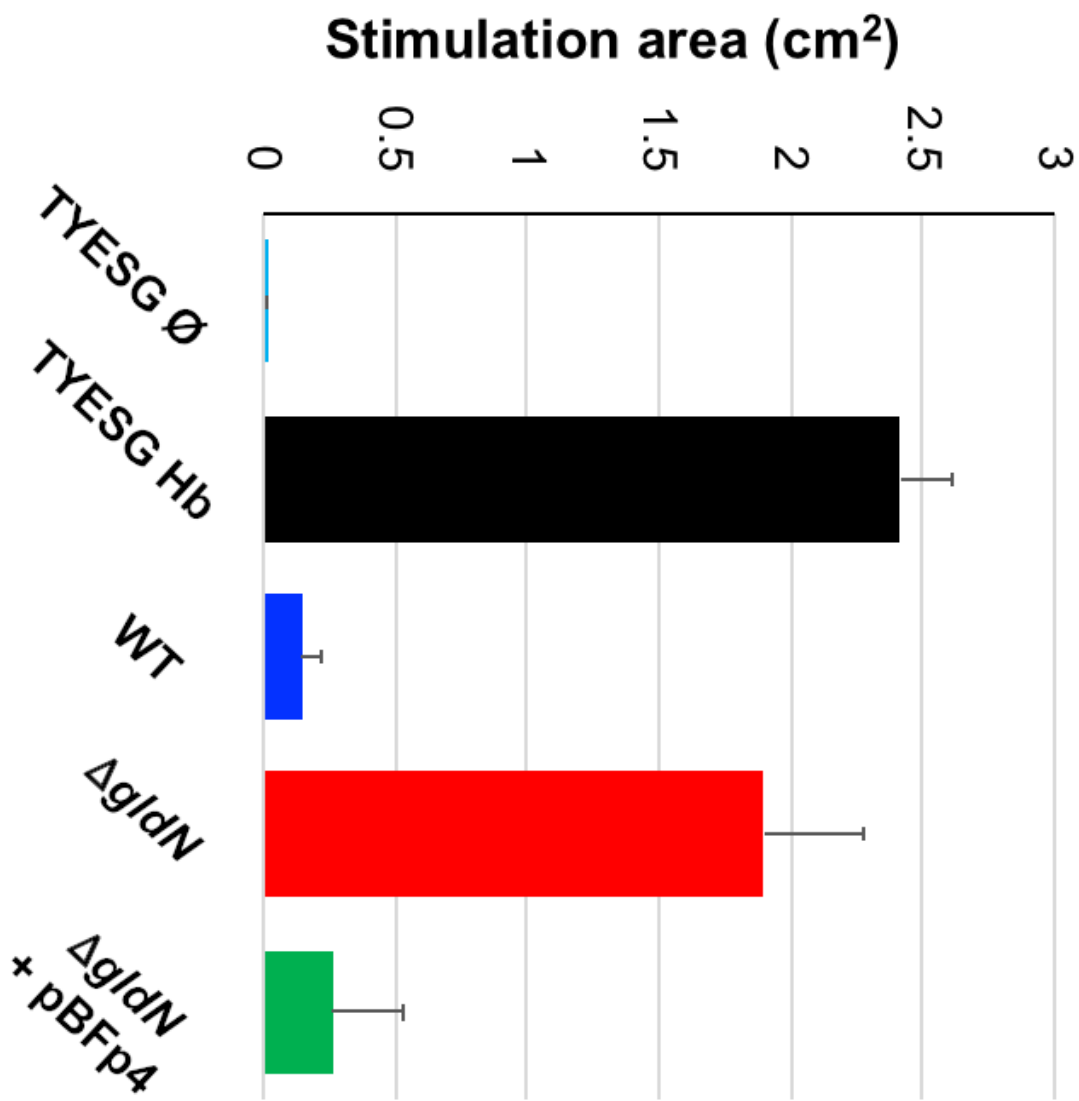

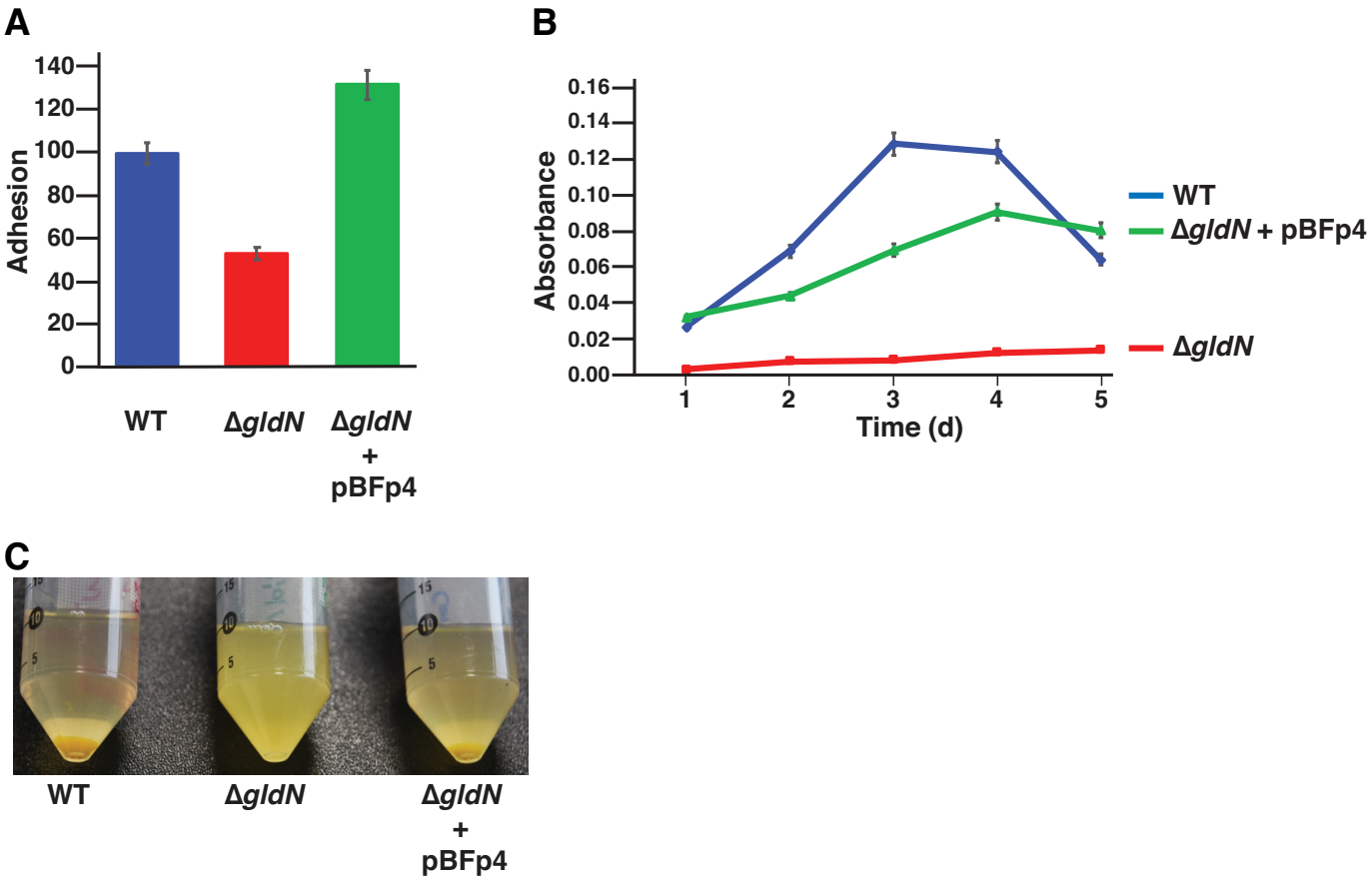

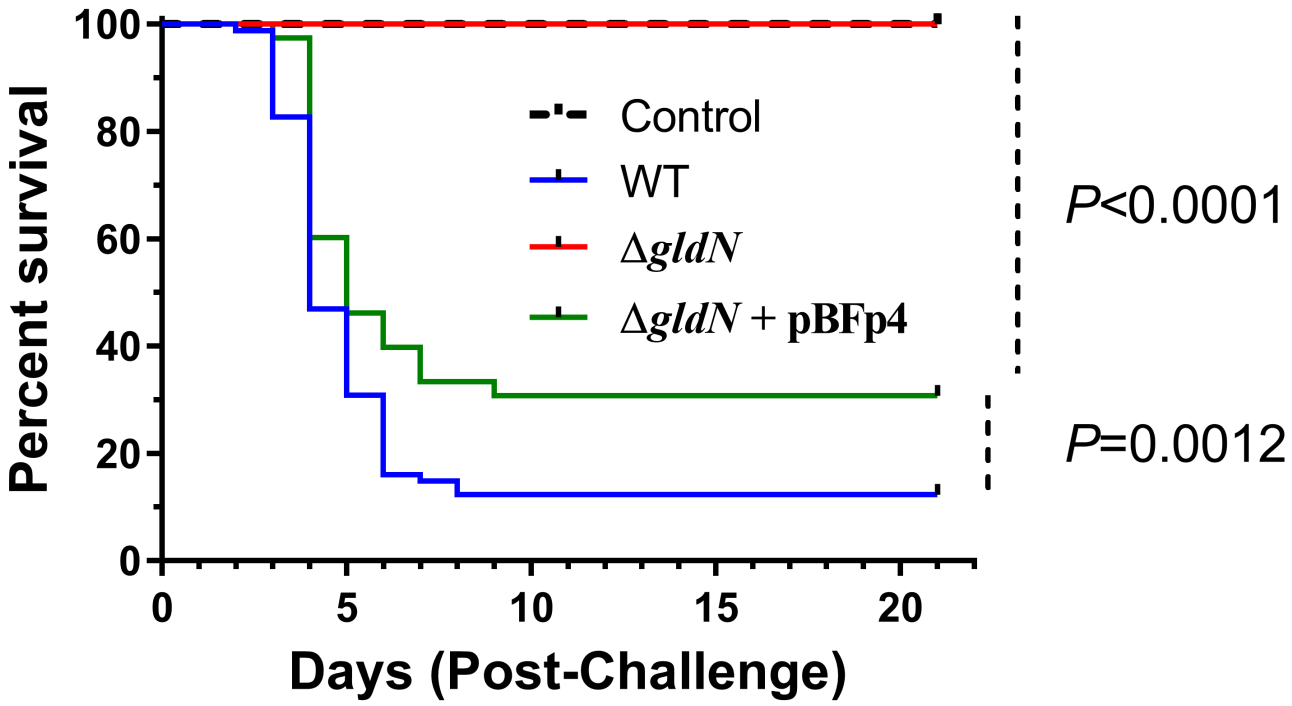

A

	CFU/ml	
	Time (hours)	
Strain	0	24
Wild-type	2.4×10^7	2.0×10^7
Δ*gldN*	2.0×10^7	1.2×10^7
Δ*gldN* + pBFp4	2.0×10^7	4.5×10^7

B

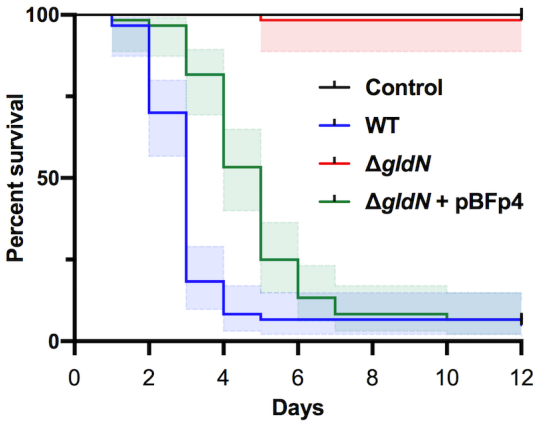

C